[American Journal of Science, Vol. 305, April, 2005, P. 259–311]

American Journal of Science

APRIL 2005

(U-Th)/(He-Pb) DOUBLE DATING OF DETRITAL ZIRCONS

P. W. REINERS*, I. H. CAMPBELL**, S. NICOLESCU*, C. M. ALLEN**, J. K. HOURIGAN*, J. I. GARVER***, J. M. MATTINSON****, and D. S. COWAN*****

ABSTRACT. Geochronology and thermochronology on detrital material provides unique constraints on sedimentary provenance, depositional ages, and orogenic evolution of source terrains. In this paper we describe a method and case-studies of measurement of both U/Pb and (U-Th)/He ages on single crystals of zircon that improves the robustness of constraints in each of these areas by establishing both formation and cooling ages of single detrital grains. Typically these ages correspond to crystallization and exhumation or eruption ages, and their combination can be used to more confidently resolve candidate source terrains, establish maximum depositional ages, and constrain the thermal histories of orogenic source regions. U/Pb dating is accomplished by laser-ablation ICP-MS in a small pit on the exterior of the crystal, and He dates are then determined on the bulk grain by conventional laser-heating and dissolution techniques. We present examples from Mesozoic aeolian sandstones, both modern and Paleogene fluvial sediments, and active margin turbidite assemblages from the Cascadia and Kamchatka margins. Important results include the fact that detritus from ancient orogens may dominate sediments thousands of kilometers away, crustal melting and exhumation appear to be spatially-temporally decoupled in at least two orogens, and first-cycle volcanic zircons older than depositional age are surprisingly rare in most settings except in the continental interior. In the case of the Kamchatkan, and possibly Olympic, turbidites, zircon He ages are partially reset. We present a method for estimating the extent of resetting of each grain and the thermal history of the sample, based on coupled (U-Th)/(He-Pb) age patterns among all the grains.

INTRODUCTION

Detrital materials in sediments and sedimentary rocks are commonly used to reconstruct timing and rates of past orogenic episodes, constrain models of paleogeography and sediment transport, establish volcanic eruptive histories, and estimate depositional ages. Although detrital studies often focus on petrographic, compositional, or other characteristics of detrital material, it is the geochronology of specific detrital minerals that provides the fundamental interpretive basis for most geologic insights about the temporal evolution of source terrains, as well as age of host units themselves. Zircon is the most commonly dated phase in detrital geochronology because it: a) is resistant to chemical and physical weathering; b) is abundant in most crustal rocks; and c) has relatively high concentrations of U and Th and low common Pb. These features make it highly suitable for geochronology and thermochronology

*Department of Geology and Geophysics, Yale University, Kline Geology Lab, 210 Whitney Avenue, New Haven, Connecticut 06511, USA; peter.reiners@yale.edu

**Research School of Earth Sciences, The Australian National University, Canberra ACT 0200, Australia

***Department of Geology, Union College, Schenectady, New York 12308, USA

****Department of Geological Sciences, University of California, Santa Barbara, Santa Barbara, California 93106, USA

*****Earth and Space Sciences, University of Washington, Box 351310, Seattle, Washington 98195, USA

by the U/Pb, fission-track (ZFT), and (U-Th)/He (ZHe) methods. Detrital zircons dated by these methods provide constraints on a wide range of geologic problems (see for example, Fedo and others, 2003, and references therein), including depositional ages (for example, Soloviev and others, 2002), provenance of the detrital material (for example, Bernet and others, 2004), and post-depositional thermal histories (for example, Garver and others, 2005). Most work on detrital zircon populations has focused on age spectra of single radioisotopic systems, such as U/Pb or fission-track, although some studies have also explored coupling age characteristics with geochemical features such as Hf or O isotopic composition (for example, Kinny and Maas, 2003; Valley, 2003, and references therein). As we show in this paper, combining geochronometric and thermochronometric ages on the same single crystals provides particularly powerful provenance information.

Conventional approaches to detrital zircon geochronology have several limitations. First, provenance constraints based on ages from single radioisotopic systems are often ambiguous because potential source terrains can have similar crystallization (that is, U/Pb) or cooling (that is, ZFT or ZHe) ages, making provenance discrimination difficult (fig. 1). Second, although the youngest zircon crystallization ages in a sedimentary rock provide an estimate of the maximum depositional age of the rock, many sedimentary units contain primarily zircon from nonvolcanic rocks, in which U/Pb ages may be considerably older than cooling and depositional ages. Third, although all dating systems are subject to one type of bias or another and to varying degrees, detrital zircon fission-track dating is subject to a sampling bias because of the difficulty in dating grains with very high track densities.

Here we describe a new method for analysis of detrital zircon geo- and thermochronology that avoids some of the limitations of conventional approaches and provides new insights into depositional systems and their sources. This technique involves the measurement of both U/Pb and ZHe ages of single zircon crystals. This approach essentially provides both high- and low-temperature ages of detrital grains, corresponding to crystallization (or high-grade metamorphism) and cooling events. In the case of first-cycle volcanic zircons, these ages are the same, but as we show, in at least some samples, including those from active margin clastic rocks, such zircons are relatively rare. Thus the combination of both crystallization and cooling ages should provide a diagnostic fingerprint of the *source terrain* from which the sediment was derived, permitting more robust provenance interpretations than possible with a single radioisotopic system, or when more than one system is applied to different grains (for example, Carter and Bristow, 2000). [Note that, following the usage of Brandon (1992), throughout this paper we use the term *source terrain* to refer to a lithologic unit with characteristic U/Pb and ZHe ages within a larger source area, rather than *source terrane*, to avoid the structural-tectonic implications of the latter term.] In this paper, we discuss the methodology of this combined technique, which we call "He-Pb double dating," provide several examples of its use in a variety of geologic settings, synthesize and discuss important features of the results, and discuss future potential and prospects for development of this and related methods in studies of detrital grains.

Methods and Special Considerations

The objective of He-Pb double dating is to measure both U/Pb and ZHe ages on the same detrital zircon crystal, and, ideally, to do this for a large number of crystals to characterize the frequency distribution of populations with distinct combinations of ages in a sediment or sedimentary rock. In some cases, several different U/Pb ages can be measured in single grains (for example, magmatic cores and metamorphic overgrowths; Campbell and others, unpublished data, 2005), and there is potential for measurement of spatially-resolved (U-Th)/He ages and "closure profiles" in single crystals (Dodson, 1986) that could yield continuous time-temperature thermal histo-

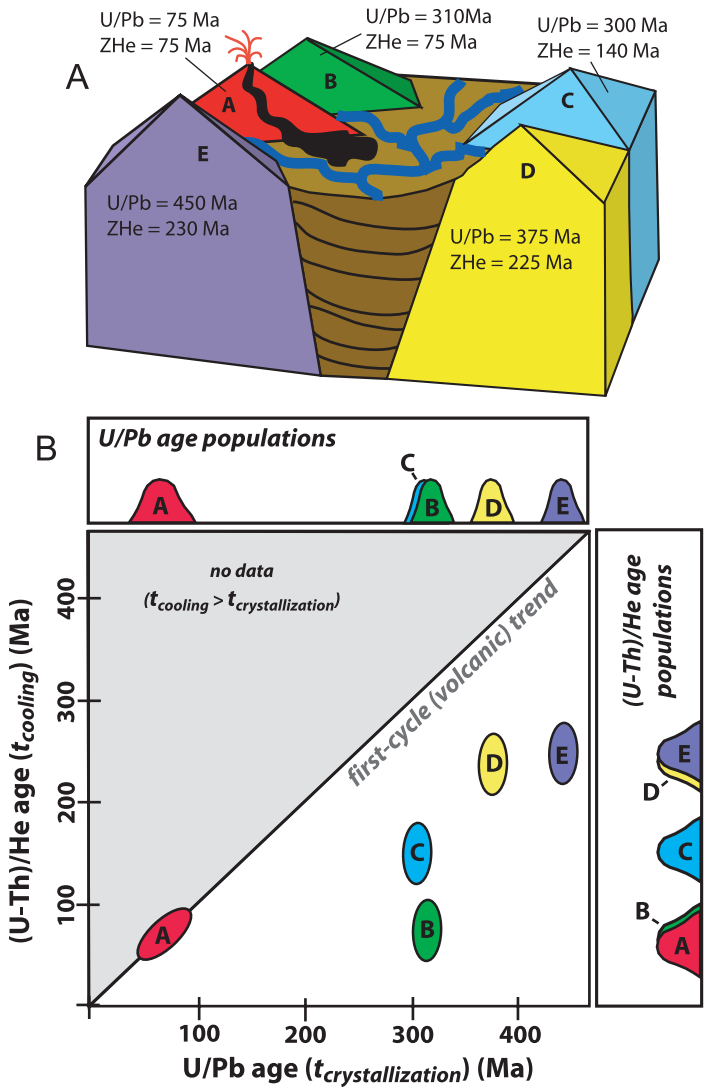

Fig. 1. Illustration of one of the principal motivations behind development of He-Pb double dating of detrital zircon. The cartoon landscape of fig. 1(A) produces detritus from 1 volcanic and 4 distinct slowly-cooled terrains, each having potentially similar U/Pb or He ages, but distinct combinations thereof. Because U/Pb dates of terrains B and C are indistinguishable, U/Pb dating alone fails to resolve these populations (same crystallization age, different cooling ages). Similarly, because He ages of terrains A and B, and D and E, are similar, (U-Th)/He dating alone fails to distinguish A from B and D from E. As shown in fig. 1(B) double dating discriminates all these sources.

ries instead of or in addition to bulk grain ages, but these developments are beyond the immediate horizon and here we focus on bulk grain age measurements.

In theory at least two different analytical procedures could be used to obtain combined He and U/Pb ages on single grains. In the first, He is extracted from a single crystal and measured as in the first step of conventional (U-Th)/He analysis, and then the abundances and/or isotopic compositions of U, Th, and Pb are quantified by thermal ionization mass spectrometry (TIMS). The He extraction step involves laser

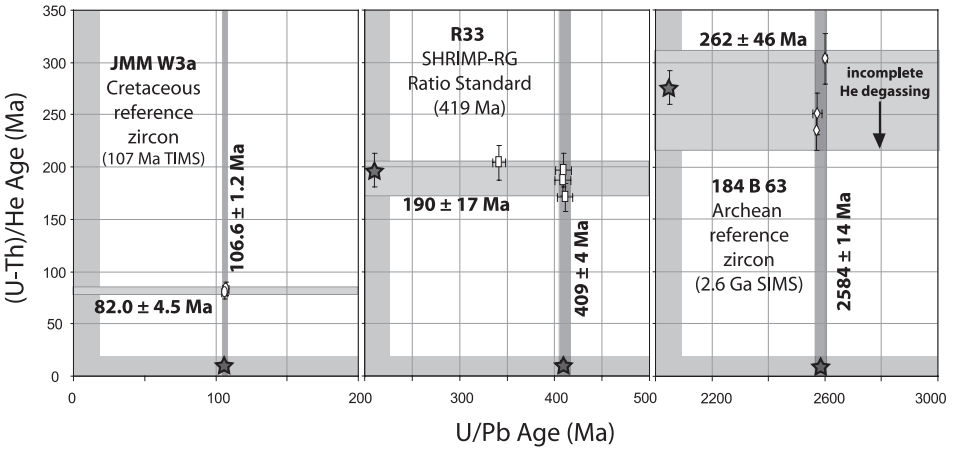

Fig. 2. Results of He-Pb dating by an alternative method than that used for most samples in this study (data are in table 1). This method involves He extraction and measurement by standard laser-heating techniques, followed by measurement of U, Th, and Pb contents and isotopic compositions by thermal-ionization-mass spectrometry (TIMS). Stars denote ages of aliquots measured as controls for either U/Pb or (U-Th)/He dating methods, without corresponding ages by the other system (gray bars). Blue and red bars are fields of variation of He (blue) and U/Pb (red) ages. Quoted ± are 1σ of age variations among aliquots. U/Pb ages are reproducible in all aliquots, despite widely varying lasing intensity during He extraction, indicating negligible Pb (or U) volatilization during He extraction. He ages of the Cretaceous and Paleozoic samples show acceptable dispersion; the range of He ages observed in the Archean zircons is attributed at least partially to variable lasing intensity during He extraction (to test effects on Pb volatilization) and incomplete He release. Despite the relatively successful demonstration of this sequence of analytical procedures for He-Pb double dating, we opted for a different method of obtaining double-dates on single zircons, largely because of the analytical care required for high-precision low procedural Pb blank analyses by TIMS.

heating of crystals inside Pt or Nb foil packets (similar to the approach described in House and others, 2000) to temperatures of approximately 1200 to 1300 °C for as many as two to four extraction steps with fifteen-minute durations. Our experiments with this double-dating analytical sequence show that even the most intense lasing required to quantitatively liberate He does not cause significant volatilization of U, Th, or Pb in zircons. We have used this procedure to double-date three different zircon standards with widely varying ages, with generally good results (fig. 2; table 1). In one case, a relatively large range of He ages to younger ages is clearly due to incomplete He extraction from zircons as part of the experimental design to evaluate lasing intensity on potential Pb loss.

The advantages of the method outlined above, in which U, Th, and Pb are measured by TIMS, include highly precise U/Pb age and U-Th concentration data, the ability to measure $^{207}Pb/^{206}Pb$ and $^{206}Pb/^{238}U$ precisely, and the ability to measure He in whole, unmodified grains as a first analytical step. The primary disadvantage of this method is the care and expense that must be taken in preparation for TIMS analysis, particularly to achieve the low procedural Pb blanks (~1 pg), required for most single-crystal age determinations. In addition, zircons cannot be pre-treated by air abrasion or acid leaching to remove potentially problematic outer portions of grains, as is commonly done in some TIMS procedures, because U-Th measurements need to be made on the same volume that contained the He. Lack of such pre-treatment probably accounts for some of the variability in the TIMS U/Pb ages (fig. 2).

An alternative procedure, and the one we followed for most samples in this study, involves first measuring U/Pb age in a small volume of a crystal by a microanalytical technique such as ion probe or laser-ablation inductively-coupled plasma mass spec-

TABLE 1

(U-Th)/He and U/Pb data for zircons dated by "reverse" double-dating, using TIMS for U/Pb.

Sample	***184 B 63, Kamchatka gneiss, ~2.6-Ga SIMS age***					
	U/Pb Control	Moderate lasing	Aggressive lasing	Moderate lasing	Weak lasing	(U-Th)/He Control
Yale ref	--	4	5	3	1	2
UCSB ref	M_02	M_04	M_05	M_07	--	--
# of grains	4	1	1	1	1	1
U (ng)	1.901	0.692	0.405	0.503	1.420	0.787
Th (ng)	0.951	0.477	0.279	0.277	0.780	0.408
^{4}He (pmol)	--	0.853	0.557	0.727	1.480	1.080
F_T	--	0.823	0.843	0.767	0.836	0.806
raw He age (Ma)	--	194	211	233	169	223
corr He age (Ma)	--	235	251	304	202	276
± (2σ) (Ma)	--	19	20	24	16	22
Th/U	0.51	0.67	0.67	0.56	0.55	0.52
Pb* (ng)	0.814	0.281	0.111	0.204	--	--
Pb_c (pg)	4.9	5.0	71.4	8.0	--	--
$^{206}Pb/^{204}Pb$	12602	4266	192	1997	--	--
$^{208}Pb/^{206}Pb$	0.14100	0.19180	0.19316	0.17501	--	--
$^{206}Pb^*/^{238}U$	0.49682 ± 0.00994	0.46341 ± 0.00927	0.45691 ± 0.00914	0.48244 ± 0.00965	--	--
$^{207}Pb^*/^{235}U$	11.83961 ± 0.23702	10.94512 ± 0.21978	10.80911 ± 0.22919	11.60868 ± 0.23470	--	--
$^{207}Pb^*/^{206}Pb^*$	0.17284 ± 0.00015	0.17130 ± 0.00031	0.17158 ± 0.00121	0.17452 ± 0.00052	--	--
$^{206}Pb/^{238}U$ age	2600.1 ± 52.0	2454.6 ± 49.1	2425.9 ± 48.5	2537.9 ± 50.8	--	--
$^{207}Pb/^{235}U$ age	2591.8 ± 51.9	2518.5 ± 50.6	2506.9 ± 53.2	2573.4 ± 52.0	--	--
$^{207}Pb/^{206}Pb$ age	2585.3 ± 2.1	2570.4 ± 4.3	2573.1 ± 16.9	2601.5 ± 7.1	--	--

TABLE 1
(continued)

Sample	*R33, Vermont; SUMAC std, 419-Ma SIMS age*					
	U/Pb Control	Moderate lasing	Aggressive lasing	Moderate lasing	Agressive lasing	(U-Th)/He Control
Yale ref	--	F,G	J	H	I	D
UCSB ref	M_06	M_08	M_21	J_07	J_08	--
# of grains	11	2	1	1	1	1
U (ng)	12.820	1.931	0.544	0.478	0.459	1.160
Th (ng)	8.760	1.526	0.504	0†	0†	0.801
^{4}He (pmol)	--	2.560	0.714	0.491	0.429	1.450
F_T	--	1	1	1	1	1
raw He age (Ma)	--	204	197	188	171	197
corr He age (Ma)	--	204	197	188	171	197
± (2σ) (Ma)	--	16	16	15	14	16
Th/U	0.67	0.77	0.90	0.00	0.00	0.69
Pb* (ng)	0.742	0.088	0.025	0.021	0.021	--
Pb_c (pg)	6.2	7.4	9.3	7.5	7.9	--
$^{206}Pb/^{204}Pb$	9079	965	273	289	272	--
$^{208}Pb/^{206}Pb$	0.21155	0.24215	0.28178	0.09869	0.09868	--
$^{206}Pb^*/^{238}U$	0.06560 ± 0.00131	0.05441 ± 0.00109	0.06556 ± 0.00131	0.06548 ± 0.00131	0.06585 ± 0.00132	--
$^{207}Pb^*/^{235}U$	0.50104 ± 0.01012	0.40043 ± 0.01046	0.54873 ± 0.02342	0.44011 ± 0.01736	0.41197 ± 0.01745	--
$^{207}Pb^*/^{206}Pb^*$	0.05540 ± 0.00015	0.05337 ± 0.00090	0.06071 ± 0.00229	0.04875 ± 0.00166	0.04537 ± 0.00169	--
$^{206}Pb/^{238}U$ age	409.6 ± 8.2	341.6 ± 6.8	409.3 ± 8.2	408.9 ± 8.2	411.1 ± 8.2	--
$^{207}Pb/^{235}U$ age	412.4 ± 8.3	342.0 ± 8.9	444.2 ± 19.0	370.3 ± 14.6	350.3 ± 14.8	--
$^{207}Pb/^{206}Pb$ age	428.2 ± 6.7	344.8 ± 40.3	628.9 ± 90.5	135.6 ± 81.6	-35.7 ± 89.6	--

TABLE 1
(continued)

Sample	*JMM W3a, Sierra Nevada, 107-Ma TIMS age*		
	U/Pb Control	Moderate lasing	Aggressive lasing
Yale ref	--	3,4,5	6
UCSB ref	M_47	M_49	M_51
# of grains	20	3	1
U (ng)	93.294	11.099	5.159
Th (ng)	25.142	3.865	1.617
^{4}He (pmol)	--	4.620	2.040
F_T	--	0.848	0.844
raw He age (Ma)	--	71	67.9
corr He age (Ma)	--	83.7	80.4
± (2σ) (Ma)	--	6.7	6.4
Th/U	0.26	0.36	0.32
Pb* (ng)	1.325	0.112	0.062
Pb_c (pg)	70.3	65.0	16.4
$^{206}Pb/^{204}Pb$	1488	205	358
$^{208}Pb/^{206}Pb$	0.08371	0.11289	0.10251
$^{206}Pb^*/^{238}U$	0.01664 ± 0.00033	0.01678 ± 0.00034	0.01663 ± 0.00033
$^{207}Pb^*/^{235}U$	0.11156 ± 0.00231	0.11339 ± 0.00518	0.10901 ± 0.00362
$^{207}Pb^*/^{206}Pb^*$	0.04863 ± 0.00026	0.04901 ± 0.00201	0.04755 ± 0.00126
$^{206}Pb/^{238}U$ age	106.4 ± 2.1	107.3 ± 2.1	106.3 ± 2.1
$^{207}Pb/^{235}U$ age	107.4 ± 2.2	109.1 ± 5.0	105.1 ± 3.5
$^{207}Pb/^{206}Pb$ age	130.0 ± 12.7	148.3 ± 98.6	76.9 ± 63.6

trometry (LA-ICP-MS), and then measuring He and U-Th contents in the rest of the grain by conventional (U-Th)/He laser heating and solution ICP-MS methods. Ion probe methods have the advantage of relatively high precision for the U/Pb measurement part of this procedure, but they also generally require a flat, polished zircon surface. Sectioning and polishing zircons for analysis introduces a minor complication for the α-ejection correction to (U-Th)/He ages, because one side of the grain is an internal surface and the remainder of the grain retains its exterior geometry, whereas the α-ejection correction is based on the dimensions and external morphology of whole, unmodified crystals. Alpha-ejection corrections can be modified to account for the post-sectioning morphology of crystals, but this requires geometric assumptions about the grains that introduce uncertainty beyond that associated with standard α-ejection corrections and analytical procedures.

Our preferred procedure for He-Pb double dating uses single-collector ICP-MS U/Pb dating of material ablated with a 193 nm laser from an ~30 μm diameter pit drilled to ~20 μm depth. Details of the method, as typically applied to He-Pb double dating, are provided in Rahl and others (2003; On-line data repository); only a few essential features are summarized here. LA-ICP-MS is performed on whole, unmodified grains attached to double-sided adhesive tape in a laser cell through which Ar-He carrier gas flows, conveying ablated material to the plasma of a quadrupole ICP-MS. The drilling rate of the 193 nm excimer laser is about 1 μm/s, and corrections are applied for down-pit elemental fractionation, instrumental mass-fractionation, and background peak intensities by use of zircon and NIST glass standards. Common Pb corrections are made by comparing thorogenic and uranogenic Pb contributions, and using the Cumming and Richards (1975) age-dependent model. Only grains meeting analytical criteria including critical thresholds of concordancy, common Pb contributions, and stability of U, Th, and Pb signals in ablated pits, are used for He dating (although occasionally crystals with obviously contrasting rim and core ages are included). The 2σ precision of this approach is typically 2 to 4 percent. The reported uncertainties include all random errors, including those associated with the standard, but do not include systematic errors such as those introduced by inhomogenity in the standard or uncertainty in its assumed isotopic ratios.

The precision of LA-ICP-MS U/Pb dating of whole unmodified zircons by these approaches is only slightly worse than typical ion probe methods, both of which are considerably less precise than typical TIMS methods. Nevertheless, the laser approach has several key advantages for He-Pb double dating. First, whole grains can be dated, and procedural Pb blank problems are largely avoided. Second, this technique enables depth profiling of several characteristics in the zircon, including U/Pb ages associated with distinct zircon growth episodes (Campbell and others, unpublished data, 2005), U-Th zonation that could produce errors in α-ejection corrections (Hourigan and others, 2005), and other trace-element features that may track crystallization environment of the zircon (for example, Ce-anomalies) or indicate inclusions such as apatite or other high-common Pb minerals. Also important for the purposes of He-Pb double dating, however, is the low cost and high sample-throughput (typically hundreds of zircons per analysis day) of LA-ICP-MS dating, permitting rapid characterization of U/Pb age spectra in detrital samples and presenting a wide sampling opportunity for targeted He age characterization of distinct U/Pb age populations.

After LA-ICP-MS dating, crystal dimensions and morphologies are measured, and crystals are loaded into ~1 mm Nb foil packets for Nd:YAG heating for He extraction. Foil packets are heated to 1200 to 1300 °C for 10 to 15 minutes, in some cases for multiple extractions to ensure >98 percent or sub-blank He release, and ^{4}He is measured by ^{3}He isotope dilution, cryogenic purification, and quadrupole mass-spectrometry and comparison to manometrically calibrated standards. Nb foil packets

are then dissolved by low U-Th blank (~1 pg) Parr bomb procedures, and U and Th are measured by isotope dilution on a single-collector sector ICP-MS (Reiners and others, 2004).

Most (U-Th)/He chronometry applications require corrections on measured He contents (or, as conventionally approximated, He ages) for relatively long stopping distances of α particles (He nuclei) in, and potentially out of, crystals. For most typical euhedral zircons, α-ejection correction has been shown to provide accurate and reproducible results, and is based on the well-known α-stopping distances in zircon, and a tetragonal prism morphology (Farley and others, 1996; Reiners and others, 2002; Farley, 2002; Tagami and others, 2003a; Reiners and others, 2004). It has been demonstrated that in some cases, systematic intracrystalline core/rim enrichment or depletion in U and Th (that is, zonation) can cause inaccurate (U-Th)/He dates (Farley and others, 1996; Farley, 2002; Tagami and others, 2003a; Reiners and others, 2004; Hourigan and others, 2005), but this is not unique to detrital zircon He dating. For combined (U-Th)/He and U/Pb dating of detrital zircons, however, a few other issues must be considered, as discussed below.

Volume, Mass, and U-Th Concentrations

The first additional consideration is not so much an adjustment to the α-ejection correction calculation as it is to the calculation of volumes and masses of dated zircons. Conventional α-ejection correction typically assumes tetragonal morphology with pinacoidal terminations. However most zircons have morphologies that more closely approximate either tetragonal prisms with bipyramidal terminations, or, in the case of many detrital zircons, prolate spheroids. Depending on how the dimensions of a grain are measured, morphological assumption of a simple tetragonal prism with pinacoidal terminations can result in a calculated crystal volume that is 20 to 100 percent larger than the actual grain volume. Because U and Th concentrations are estimated from masses determined from these volumes, this results in unrealistically low U and Th concentration estimates. Note however, that because He ages are calculated on the basis of measured molar contents (not concentrations) of U, Th, and ^{4}He, this volume estimate does not affect calculated ages.

Motivated in part by our observations that masses calculated using a morphology of tetragonal prisms with pinacoidal terminations produced U and Th concentrations systematically lower than those measured by U/Pb dating, we developed new procedures for volume and mass estimates that approximates grains as either tetragonal prisms with bipyramidal terminations or prolate spheroids, depending on the observed morphology of the grain. Aside from using these models to calculate volume and mass, we also use these more realistic morphologies for calculating α-ejection corrections for zircon (for example, Hourigan and others, 2005). However, it is important to note that because α-ejection corrections are primarily determined by surface-area to volume ratios (not simply volume), age corrections are typically within 1 percent of those calculated using a more simple morphology. In effect, for most grains, using conventional versus more realistic crystal morphologies in calculating volumes/masses and α-ejection corrections causes a very significant difference in estimated U and Th concentrations, but only a very slight age difference.

Our modified methods for volume/mass and α-ejection corrections first assign an assumed morphology of either tetragonal prism with bipyramidal terminations or prolate spheroid, based on dual-perspective digital images of a grain. For tetragonal prisms we measure two mutually perpendicular prism half-widths perpendicular to the c-axis (r_1, r_2), a c-axis parallel length (l), and two "tip" heights corresponding to the two pyramidal terminations (h_1, h_2). Minor irregularities such as chips or dimples are generally ignored. The volume (V_z) and surface area (SA_z) of this morphology are given by:

$$V_z = 4r_1r_2[(l - h_1 - h_2) + \tfrac{1}{3}(h_1 + h_2)] \quad (1)$$

and

$$SA_z = 4(l - h_1 - h_2)(r_1 + r_2) + 2r_1a + 2r_2b \quad (2)$$

where a and b are related to the slant heights of the pyramidal terminations,

$$a = \sqrt{h_1^2 + r_2^2} + \sqrt{h_2^2 + r_2^2} \quad (3a)$$

$$b = \sqrt{h_1^2 + r_1^2} + \sqrt{h_2^2 + r_1^2} \quad (3b)$$

For grains more closely approximating prolate spheroids (for example, highly abraded detrital grains), an average equatorial radius r, and length l, are determined, and the volume (V_{ps}) and surface area (SA_{ps}) are given by:

$$V_{ps} = \tfrac{2}{3}\pi r^2 l \quad (4)$$

and

$$SA_{ps} = 2\pi r^2 + \left[\frac{2\pi r(l/2)}{\sqrt{(l/2) - r^2}}\right]\sin^{-1}\left[\frac{\sqrt{(l/2) - r^2}}{(l/2)}\right] \quad (5)$$

For U and Th concentration estimates, volume is converted to mass by assuming a zircon density of 4.6 g/cm^3. For α-ejection corrections, the surface-area-to-volume ratio β, and the measured Th/U of the crystal are used in second-order polynomials to calculate the fraction of alphas retained in the crystal for both the U and Th decay series. The polynomials are derived from Monte Carlo simulations of α-ejection from grains with the assumed morphologies (Farley, 2002; Hourigan and others, 2005). For a model zircon with a morphology of a tetragonal prism with bipyramidal terminations, the two factors in each of our polynomials are slightly different from those of Farley (2002). However, as long as the βs are calculated on the basis of the appropriate crystal morphologies, they produce α-retention factors (F_Ts) within 1 to 2 percent of those with the Farley (2002) *calculated with the same* β, for the vast majority of crystal morphologies and dimensions encountered. As noted by Farley and others (1996), for most crystals, surface-area to volume ratio, not the specific geometry of the crystal, exerts the dominant control on α-ejection. Because of this, for grains with prolate spheroid geometries, we use Farley's (2002) polynomial relating β to α-ejection factors, but we use the prolate spheroid geometry for calculating β.

Figure 3 compares U and Th concentrations and Th/U for bulk zircons determined by (U-Th)/He methods, and for the ~20 μm deep pits on the rims of crystals determined by the LA-ICP-MS U/Pb dating. It is worth noting again that while U and Th concentrations by these methods provide an interesting cross-calibration comparison, neither (U-Th)/He nor U/Pb ages are calculated using concentrations; both methods calculate ages based on ratios of moles of parent and daughter nuclides in analyzed volumes. Note that this approach is distinct from Ar/Ar and fission-track dating, for which ages rely on reference to age standards. In the case of He dating, the estimated concentrations are based on estimated volumes, and in the case of U/Pb dating concentrations are determined by comparison with standards of known concentrations. There is not necessarily an expectation that U and Th concentrations in the outer 20 μm of a grain and in the whole grain should be equal, as U and Th zonation is common in zircon and can be pronounced in some cases. Nonetheless, the agreement of bulk and rim U-Th concentrations is within a factor of two for the vast majority of grains, with no evidence of a systematic offset in concentration as determined by these

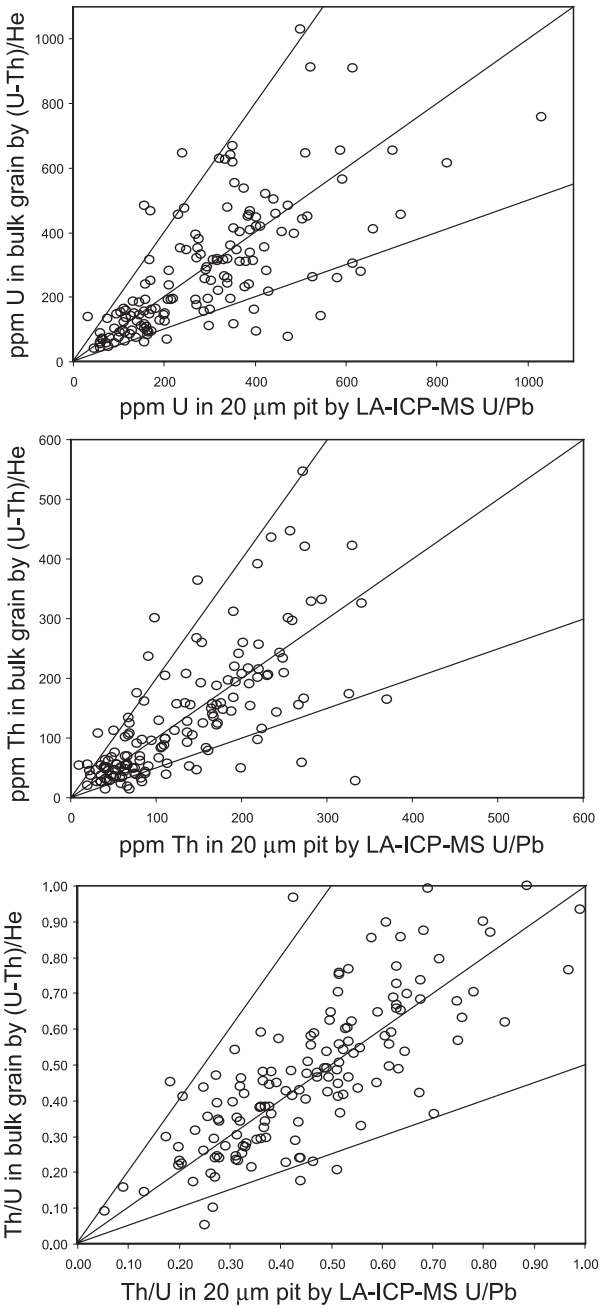

Fig. 3. U and Th concentrations and Th/U for bulk crystals by He dating methods (y-axis) and in outer 20 μm pits of zircons by LA-ICP-MS U/Pb dating methods (x-axis). Thin solid lines are trends of 1:1, 2:1, and 1:2 concentrations or concentration ratios. Neither dating method uses absolute concentrations of parents to calculate ages, and U-Th concentrations in the He method are estimated by grain dimensions and assumed morphologies and densities, so these estimates are not important for actual ages. Nonetheless, there is no indication of a systematic inaccuracy between the methods. The fact that the vast majority of bulk grains have similar U-Th concentrations within about a factor of two as the outer 20 μm of the grain also does not indicate systematic or extremely strong bias in He ages from parent nuclide zonation and its effect on α-ejection correction. In all plots a few (<4) symbols are not shown because of extreme values that would shrink the plot scales. Thirty of the points in each panel are zircons from the Missouri river (Reiners and others, unpublished data), which are similar to all the other samples.

techniques (fig. 3). A factor of two difference in the U-Th concentration, determined from the bulk grain and ~20 μm rims methods, can result in (U-Th)/He age inaccuracies, arising from U-Th zonation, of up 10 percent, but will probably be significantly less in most cases. As shown in Reiners and others (2004) and Hourigan and others (2005), although the (U-Th)/He age inaccuracy resulting from U-Th zonation depends on the distance of concentration contrasts relative to the crystal rim, contrasts of a factor of two lead to maximum age inaccuracies of less than ~7 percent.

Natural Abrasion of Zircon Rims

Another methodological consideration is necessary for (U-Th)/He dating of detrital zircons that have been significantly abraded during transport prior to deposition. Natural abrasion during transport may remove part or all of the outer ~20 μm rim of crystals that is depleted in He because of α-ejection. Thus applying the standard α-ejection correction to He ages of detrital grains that have experienced significant abrasion following closure of the (U-Th)/He system will result in overcorrection, and corrected ages that are too old. The proper α-ejection correction depends on several factors, most importantly the fraction of the He-depleted rim lost by abrasion, and the amount of time following abrasion relative to the pre-transport and pre-depositional age. An additional factor is the duration of abrasion, relative to the zircon's He age, which for simplicity we assume here to be negligibly short. We also assume no resetting of the (U-Th)/He age following abrasion and deposition.

An extreme example is a recently deposited zircon that lost its entire He-depleted rim during an episode of transport that is short relative to the He age of the crystal (for example, a highly-rounded zircon in modern alluvium, originally derived from crystalline basement). Assuming no additional complicating factors such as extreme U-Th zonation or diffusive rounding of the He profile, this crystal requires no α-ejection correction at all. However, if this same zircon then resides in a sedimentary rock for a duration of time that is significant compared with its pre-depositional He age, then an α-ejection correction must be made, but only for the time since deposition (Rahl and others, 2003).

In our experience, few zircons in sediment or sedimentary rocks that we have dated by this technique show degrees of rounding sufficient to assume complete removal of the α-ejection rim. Many show slight rounding at the apices of crystal faces, but it is difficult to assess the impact this would have on α-ejection corrections, though we expect it to be minor compared with other sources of uncertainty. In such cases we apply the standard α-ejection correction. Although this may cause some overestimation of He ages, in ambiguous cases we generally adopt asymmetric He age uncertainties, allowing for younger ages if no, or only post-depositional (as below) α-ejection corrections are applied.

In their He-Pb double-dating study of the Navajo sandstone, Rahl and others (2003) noted that nearly all zircons in this aeolian deposit were very highly rounded, and many of them were nearly spherical. These authors developed a method for post-depositional α-ejection correction, and assessed both the conditions under which it would apply and the deviations of He ages resulting from this and the standard α-ejection corrections. For the case of the ~190-Ma Navajo sandstone and the common zircons with 0.9 to 1.3 Ga (U-Th)/He ages, this deviation could be 30 percent or more (Rahl and others, 2003). Their equation for a modified post-depositional α-ejection corrected age A_c, is:

$$A_c = A_d(1 - F_T) + A_m \tag{6}$$

where A_d is the depositional age of the host sedimentary rock, F_T is the standard α-ejection correction factor as described above, and A_m is the measured age as determined from relative abundances of parent and daughter nuclides.

Old Age Limitations to Zircon (U-Th)/He Dating

Fission-track dating of detrital zircon has a well-known potential sampling bias, because of the inability to date highly damaged grains with high track densities. The zircon (U-Th)/He system is also known to be limited by the effects of radiation damage, although to lower degrees, and for different reasons. In the case of zircon He dating, the problem is that very old grains with high U (and Th) concentrations and long-term low-temperature histories may have accumulated sufficient damage to significantly affect crystallinity and therefore He diffusivity at low temperatures, leading to geologically meaningless ages. Two independent lines of evidence, together with mineralogic considerations, constrain conditions under which zircon He ages may be suspect due to radiation damage effects.

Reiners and others (2004) showed that zircons with U concentrations in excess of ~900 ppm (and Th ~400 ppm) and He ages as old as ~440 Ma show He diffusion characteristics in cycled step-heating experiments that are essentially identical to those of zircons with much younger ages and much lower U concentrations (for example, 120 Ma and 80 ppm U). This observation suggests that accumulation of radiation damage at least up to ~1.5 x 10^{18} α/g, in zircons held at temperatures below ~200 °C for at least ~440 Myr, does not cause significant changes to He diffusion.

These He diffusion results are consistent with results of studies showing a relatively abrupt change in unit cell properties and other characteristics of zircons at accumulated radiation dosages of about 2 to 4 x 10^{18} α/g, with little significant change at lower dosages. This threshold level of radiation dosage has been suggested to correspond to a fundamental change in macroscopic and spectroscopic properties of zircon resulting from a percolation threshold of crystallinity brought on by overlapping α decay damage zones (for example, Holland and Gottfried, 1955; Zhang and others, 2000; Nasdala and others, 2001; Ewing and others, 2003).

This interpretation that He diffusion in zircon is significantly affected only above accumulated radiation dosages of about 2 to 4 x 10^{18} α/g is supported by zircon He ages of crystals with similar ages and thermal histories but strongly contrasting U-Th concentrations. Nasdala and others (2004) showed that a suite of detrital zircons with nearly identical U/Pb ages presumably derived from a common (or similar) source(s), but widely ranging U and Th concentrations (U = 290-5600 ppm; Th = 30-800 ppm), had consistent and highly reproducible (U-Th)/He ages of 443 ± 18 (2σ) Ma, as long as the α-dosage, calculated using either He or U/Pb ages, did not exceed 2 to 4 x 10^{18} α/g. Zircons with radiation dosages exceeding this amount showed much younger He ages, and exhibited anomalously high He diffusivity at room temperature. This same general phenomenon in Sri Lankan and Canadian zircons was demonstrated by Hurley (1954) and Hurley and others (1956).

More recent results from zircons from a wide range of settings, including samples from the Canadian shield, the Gold Butte block of southern Nevada, and Archean gneiss of the Wyoming craton all support the hypothesis that He diffusion at relatively low temperatures is not affected by radiation damage up to ~2 x 10^{18} α/g, but is strongly affected at doses above this level. As shown by Nasdala and others (2001) and Nasdala and others (2004), spectroscopic characteristics of many zircons suggest that they have measured radiation damage that is much less than would be expected from their U-Th concentrations over a duration of time equal to their U/Pb (that is, formation) ages. This is likely due to annealing of the damage at elevated temperatures (for example, Garver and Kamp, 2002). Thus radiation damage effects on He diffusion and (U-Th)/He ages cannot necessarily be calculated solely from U/Pb ages. Zircons must accumulate radiation damage at relatively low temperatures for it to strongly affect He diffusion and ages. The precise relationship between thermal history and retention of radiation damage that can affect He diffusion is not known at present.

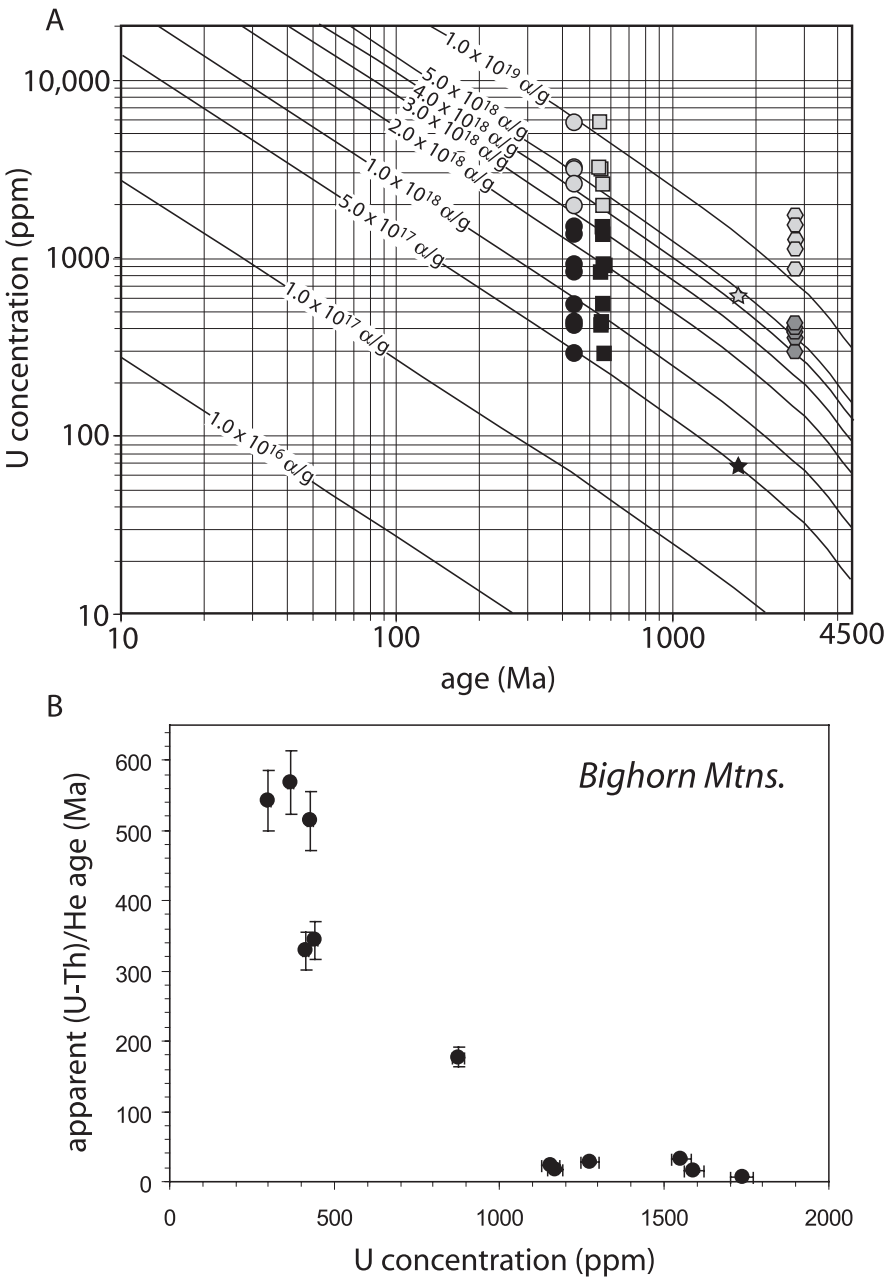

Fig. 4. (A) Contours of α-dosage as a function of age and U concentration, assuming Th/U = 0.5, a typical value for zircon. Also shown are zircons from the detrital Sri Lankan suite studied by Nasdala and others (2004) (circles), two zircons from the Canadian shield (stars), courtesy of Rebecca Flowers, MIT, and a suite of zircons from the Shell Canyon region of the Bighorn Mountains (octagons; unpublished data) (samples BH-12 and BH-17 of Reiners and Farley, 2001). Sri Lankan zircons are shown for both He age (442 Ma) and U/Pb age (555-560 Ma). Canadian shield and Bighorns zircons are shown for $^{40}Ar/^{39}Ar$ biotite cooling ages of 1.76 Ga and 2.8 Ga, respectively. Black symbols denote samples yielding ZHe ages that are reproducible and consistent with other thermochronologic constraints, implying insufficient accumulated radiation damage to affect the He age. Light gray symbols represent samples with anomalously young and unreproducible He ages, attributed to the effects of high radiation damage. Darker gray symbols for the low-U Bighorns samples denote samples with ages between 330-570 Ma; lighter gray symbols denote samples with ages between 7-178 Ma. None of these samples

However, it is likely that temperatures of about 200 to 300 °C are sufficiently high to prevent complete radiation damage accumulation (Ewing and others, 2003).

Some limits on the expected effects of radiation damage and the viability of meaningful zircon (U-Th)/He ages can be made based on combined U-Th concentration and age, and on the assumption that there is full retention of all damage at low temperatures. Figure 4 shows contours of radiation damage that would be accumulated, assuming full retention at low temperature, for various combinations of U concentration (assuming a typical Th/U of 0.5) and age. Also shown are ages and U concentrations of three different suites of single-grain zircon analyses. Zircons from the Sri Lankan detrital suite of Nasdala and others (2004) have highly reproducible ages for crystals with less than 2.5 x 10^{18} α/g, whereas ages are much younger and poorly reproducible for crystals with dosages greater than 3.0 x 10^{18} α/g (dosages calculated for the 442 Ma age of the low-U crystals). Two zircons from different but nearby samples in the Canadian shield with ~1.9 Ga crystallization ages and U concentrations of 66 ppm and 612 ppm, show He ages of 1.76 Ga and 69 Ma, respectively. The biotite $^{40}Ar/^{39}Ar$ age for this area is 1.76 Ga (R. Flowers, personal communication), suggesting that the 1.76 Ga zircon He age records a real cooling event, and the 69-Ma age is geologically meaningless. Because of their strongly contrasting U concentrations, the 1.76-Ga radiation dosages for these two crystals do not tightly bracket the apparent threshold dosage for enhanced He loss, but they do suggest a critical threshold less than 4.3 x 10^{18} α/g.

The third suite of zircons that sheds some light on the relationships between radiation damage and He retention is from the Bighorn Mountains of Wyoming (fig. 4). These zircons are from two different hand-samples of a 2.8-Ga granitoid in the Shell Canyon location where modeling of crystal-size-age relationships in apatite indicates residence at temperatures less than ~60 to 80 °C during the last 600 Myr (Reiners and Farley, 1999). (U-Th)/He ages of these zircons show a clear inverse correlation with bulk grain U concentration, with a maximum age of ~570 Ma for grains with ~300 ppm U, and a minimum apparent age of 7 Ma for grains with 1740 ppm U (fig. 4B). Unfortunately grains with less than about 300 ppm U have not been analyzed, and there is no obvious inflection in the age-U concentration curve that could be used to identify old and invariant ages in grains with low U concentrations, as in the Sri Lankan suite (Nasdala and others, 2004). Because the age of cooling through low-temperatures is not known in this case, it is not possible to calculate accumulated radiation dosages for these grains. If these samples cooled through a temperature corresponding to that of radiation damage accumulation at 2.8 Ga [for example, the biotite K/Ar age; Heimlich and Banks (1968); Heimlich and Armstrong (1972)], then even the lowest-U crystal (~300 ppm) would have accumulated ~4.0 x 10^{18} α/g of damage. If the critical threshold for accumulated radiation damage is ~2-3 x 10^{18} α/g, as interpreted from the Sri Lankan zircons, then all the zircons would be damaged beyond the point of significant effects on low-temperature He diffusion, which is consistent with the lack of invariant old He ages at the lowest U contents measured. Thus it is likely that in this case none of these zircons preserve a conventionally interpretable (U-Th)/He age (for example, one corresponding to cooling through approximately 180 °C).

In summary, although these data illustrate some uncertainty surrounding the relationships among thermal history, radiation damage, and He age, they illustrate at

---

have reproducible ZHe ages at any U concentration, suggesting that they have all accumulated radiation damage sufficient to cause low-temperature He loss and anomalously young ZHe ages. (B) ZHe age as a function of U concentration for the Bighorns samples, showing a good anticorrelation suggesting a radiation damage control on apparent age. Also see Hurley (1954) and Hurley and others (1956).

least two important points. The first is an empirical indication of an upper age limit to zircon He dating that is radiation-damage dependent. Zircons with high accumulated radiation dosages are susceptible to enhanced He diffusion at low temperatures. However, because radiation damage can be annealed at moderate temperatures (c. 300 – 400 °C; for example, Nasdala and others, 2001, 2004; Garver and Kamp, 2002; Ewing and others, 2003; Rahn and others, 2004), zircon must reside at sufficiently low temperatures (<200-300 °C) to accumulate significant radiation damage. Naturally, this means that the U/Pb age is only the maximum possible duration for accumulation of radiation damage affecting He diffusion. The appropriate threshold temperature is not well known but, based on the data shown here, it is likely at least as high as the zircon He closure temperature. If the ages (Nasdala and others, 2004) and He diffusion characteristics (Reiners and others, 2004) of the Sri Lankan zircons are used as guide, then accumulation of more than about 2-3 x 10^{18} α/g of radiation damage at temperatures below about 200 °C is sufficient to significantly affect He diffusion properties and cast doubt on a zircon He age as representing any geologically significant cooling event or thermal history. Unfortunately, in some situations it may be difficult to know if a zircon has accumulated this much damage, because if it has, the resulting enhanced low-temperature He diffusion will cause the He age to be "too-young."

For practical purposes then, even though the U/Pb age may not be appropriate for calculating accumulated radiation dosage, we recommend caution when attempting interpretation of zircon He ages for which the U-Th concentrations and U/Pb ages indicate even a potential for damage accumulation as high as ~2-3 x 10^{18} α/g (assuming low-temperature residence for the full lifetime of the zircon to present). For zircons with relatively low U concentrations of ~100 ppm, this corresponds to 3 to 4 Ga; for zircons with relatively high U concentrations of ~1000 ppm, this corresponds to 530 to 770 Ma. A recent compilation of 650 dated zircons in the Yale lab suggest an average U concentration of about 350 ppm [a literature survey by Garver and Kamp (2002) indicated an average of 419 ppm U in zircon], which would require about 1.4 to 2.0 byr at low-temperature conditions, to reach the potential radiation damage threshold. In our experience, in most cases zircons with this much accumulated damage are easily identified by red or brown colors, and, in some cases, optical isotropy and detectable *in vacuo* He loss at room temperatures.

Finally, we note that for some samples there is a potentially useful but as yet unexplored signal in the relationship between zircon He age and radiation damage. If the relationship between radiation damage and He diffusivity could be quantified and parameterized through diffusion experiments on specimens with moderate through severe damage, then the specific relationship between age and U-Th contents could potentially be used to constrain the thermal history of these grains at temperatures lower than the nominal zircon He closure temperature.

Statistical Considerations with Detrital Zircons

Although the use of detrital zircons in provenance analysis, depositional age constraints, and other applications has a long history (for example, Fedo and others, 2003, and references therein), relatively few studies have focused on quantitative statistical evaluation of interpretations from detrital zircon datasets (Dodson and others, 1988; Sambridge and Compston, 1994; Sircombe, 2000; Sircombe and Hazelton, 2004; Vermeesch, 2004; Andersen, 2005). Two recent papers (Vermeesch, 2004; Anderson, 2005) focused largely on the question of how many zircons from a given detrital population must be dated in order to find at least one grain representing a source with a distinctive age signature. These studies emphasized that in general, datasets with about 100 randomly selected grains will typically run a significant risk of missing sub-populations comprising less than about 10 percent of the overall popula-

tion, and that apparent relative abundances of each sub-population may be significantly biased. Andersen (2005) also discussed the perils in interpreting ancient sediment-source mass fluxes based on detrital zircon populations, and questioned the use of minimum ages of detrital zircons as maximum depositional ages of their sedimentary hosts.

In this paper we have not quantitatively (that is, statistically) evaluated the extent to which He-Pb double dating, or any other method capable of identifying two distinct fingerprints for each grain, affects provenance, mass-flux, or depositional age interpretations. The examples described here use relatively small numbers of zircons and are clearly subject to interpretational uncertainties afflicting small datasets. Provenance and other interpretations made here are largely qualitative and do not claim to rule out contributions from candidate source terrains or age groups with any statistical rigor. As discussed in both Vermeesh (2004) and Andersen (2005), small datasets such as the ones shown here serve primarily to identify major age sub-populations and their likely sources and other geologic implications, even if not ruling out the presence of minor ones.

While our examples are clearly subject to the limitations of small datasets, we contend that He-Pb double dating in general provides significant interpretational advantages over single-method dating of detrital zircons, at least in some cases, if only because source regions may be difficult to distinguish based on either crystallization or cooling ages alone, whereas combinations of both are more likely to be unique. Another feature of He-Pb double dating is that, at least with the methods we have used in this study, in a given amount of time, many more zircons can be analyzed for LA-ICP-MS U/Pb ages than for (U-Th)/He ages. This means that rather than randomly selecting grains for both dating techniques, a relatively small number of grains can be strategically selected from larger populations of U/Pb ages in order to systematically characterize cooling ages of individual U/Pb-age sub-populations. This approach can be used strategically to resolve ambiguities arising from single-system age spectra, or test hypotheses based on U/Pb data alone. This approach, while potentially powerful for resolving provenance issues, may not lend itself easily to statistical tests of interpretations, because of the additional bias involved in selecting grains for He dating from the U/Pb populations. Nonetheless, future studies may find value in exploring statistical means of resolving candidate source terrains based on two-dimensional age criteria.

Finally, we suggest that the He-Pb double dating may ameliorate some of the problems associated with estimating maximum depositional ages from minimum ages of detrital zircons. Andersen (2005) noted that (for single-system dating) such constraints are subject to large uncertainties, especially in cases of small datasets in which minor sub-populations may be missed, or where sediments were deposited far from active zircon-producing terrains (for example, magmatic areas). He-Pb double dating offers the opportunity to improve the reliability of maximum depositional age constraints by comparing cooling ages of those grains with the youngest U/Pb ages. If partial resetting of the zircon He system in the sediment or sedimentary host can be ruled out, then a cooling age equal to the minimum U/Pb age provides evidence for a volcanic source. This is still not a guarantee of the depositional age, but depending on the age resolution required, and combined with other information, such as zircon morphology and tectonic inferences, it strengthens the claim. Alternatively, if the cooling age is significantly younger than the minimum U/Pb age, this at least improves the maximum depositional age constraint.

Results of regional He-Pb double-dating studies and discussion

Here we present new data and review one set of previously published results from several studies of He-Pb double dating of zircons from sediments or sedimentary rocks.

The objective of this section is to demonstrate a range of applications and types of geologic constraints the method provides. Besides the requisite concordance on quickly-cooled volcanic standards in the first example, these results show several important features of He-Pb zircon data. The second example shows source discrimination in provenance analysis of an aeolian sandstone from the southwestern U.S. The third shows the surprisingly large contribution of first-cycle volcanic detritus from the western U.S in Mississippi River sediment, and a relative lack of detritus from the eastern U.S. The fourth example illustrates the use of He-Pb double dating to estimate depositional age of an early Tertiary paleofluvial deposit in Oregon, and the orogenic and magmatic history of its sources. The fifth example, from the Olympic mountains also attempts to constrain depositional age, but more clearly shows an apparent decoupling between episodes of zircon formation (crustal melting) and exhumation in the Pacific northwest. Finally, the last example, a synorogenic flysch of the Kamchatka peninsula, illustrates the effects of partial resetting on zircon He ages in He-Pb double dating, and the constraints it provides on burial thermal histories.

Fish Canyon Tuff - Quickly-Cooled Volcanic Age Standard

Two of the initial concerns with using laser ablation to measure U/Pb ages in pits on crystals prior to He measurement were the potential for laser-heating induced He loss, and the potential effects of pit removal on α-ejection corrections. Such effects would be evident in He ages of double-dated zircons of a suitable standard, such as those from the well-known Fish Canyon Tuff (FCT). There is some debate as to the crystallization and cooling ages of different phases in the FCT (for example, Lanphere and Baadsgaard, 2001; Schmitz and others, 2001; Schimtz and others, 2003), with zircon analyses in different labs yielding TIMS ages of 28.48 ± 0.06 Ma (2σ) (Schmitz and Bowring, 2001) and 27.52 ± 0.09 Ma (Lanphere and Baadsgaard, 2001), and some lower closure-temperature systems yielding ages similar to the latter age (Lanphere and Baadsgaard, 2001). In any case, this range is well within the observed two standard deviations of FCT (U-Th)/He ages (9%). Figure 5A shows combined U/Pb and (U-Th)/He ages for 19 crystals of Fish Canyon Tuff zircon dated by our procedures. The mean U/Pb age for these crystals is 28.8 Ma, with two standard deviations of 1.7 Ma (6%), and the mean (U-Th)/He age is 28.6 Ma, with two standard deviations of 2.7 Ma (10%). The He ages of the double-dated grains compare well with those of 83 grains from the same sample that were dated only by (U-Th)/He, which show a mean of 28.3 Ma, with two standard deviations of 2.6 Ma (9%) (fig. 5B). We conclude that these data show that laser ablation of a 20-μm pit for the U/Pb dating does not cause significant He loss from the grain, nor does it significantly modify the α-ejection correction.

Navajo Sandstone - Aeolianite With Distal Source

Figure 6 shows combined (U-Th)/He and U/Pb ages of seventeen zircons from two samples of the ~190 Ma Navajo sandstone from southern Utah, originally reported by Rahl and others (2003). The Navajo-Nugget-Aztec sandstone represents remnants of one of the largest known erg deposits, with an estimated original areal extent as large as $\sim 7 \times 10^5$ km^2 (Marzoff, 1988). Paleocurrent indicators suggest an immediate derivation of the sand from the north-northwest, but the ultimate source of the detritus has been debated (Kocurek and Dott, 1983; Peterson, 1988; Marzoff, 1988; Dickinson and Gehrels, 2003).

He-Pb double-dates of the Navajo zircons show that most grains fall into one of three populations: a) those with U/Pb dates between 400 to 600 Ma and slightly younger He dates between ~200 to 500 Ma; b) those with U/Pb dates of 900 to 1200 Ma and He dates similar to the previous group, of 250 to 500 Ma; and c) those with U/Pb dates of 2.6 to 2.8 Ga and He dates similar to but slightly older than the U/Pb dates of the previous group (1.1-1.4 Ga) (fig. 6). Rahl and others (2003) interpreted

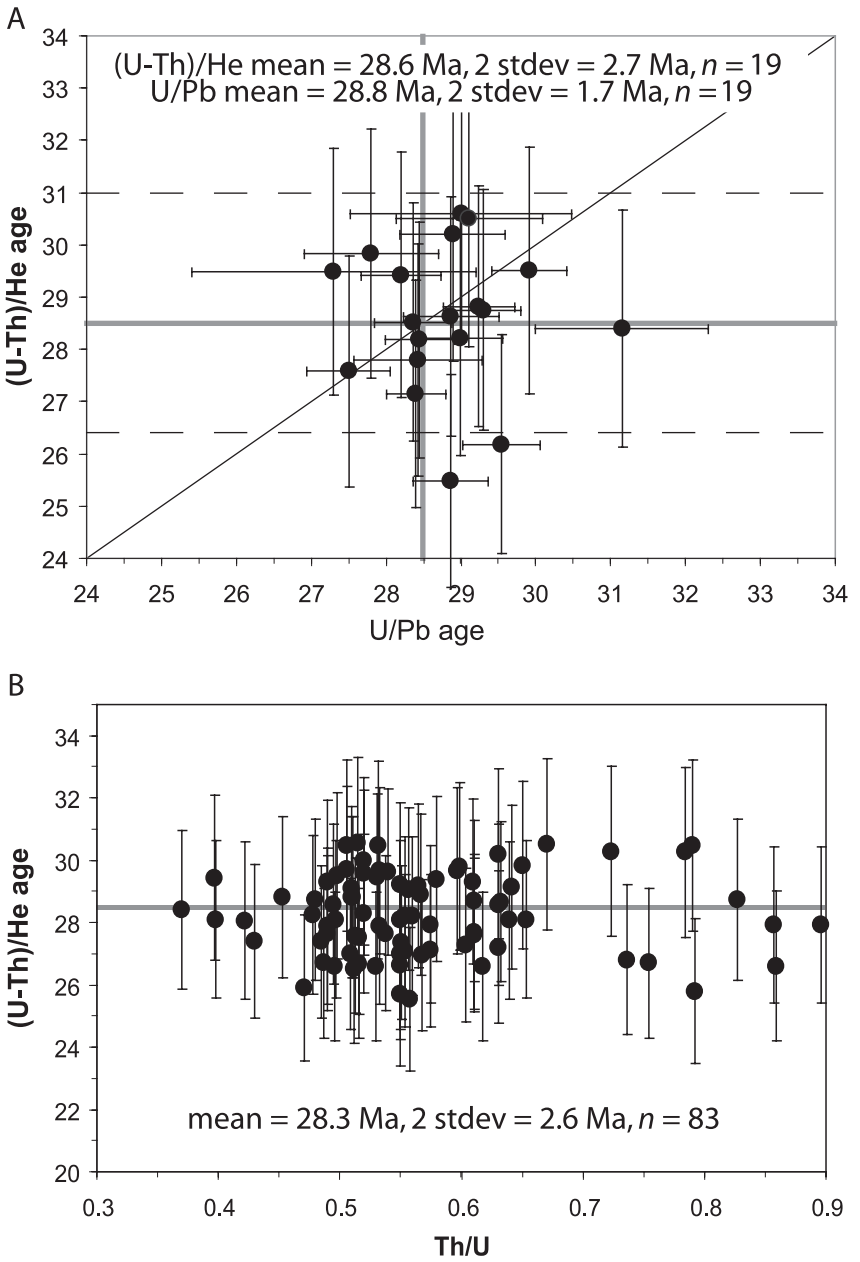

Fig. 5. Fish Canyon Tuff ages by He-Pb double-dating methods (A) and by conventional (U-Th)/He dating methods (B) performed at Yale. The mean and standard deviation of ZHe ages of zircons dated by both methods are similar to those of conventionally dated zircons, demonstrating no significant effects of the LA-ICP-MS U/Pb procedures on ZHe ages of grains.

these combinations of high-temperature (crystallization) ages and cooling ages (through ~180 °C) as: a) zircon that formed and cooled in the Appalachian orogeny; b) zircon formed in the Grenville orogeny and cooled in the Appalachian orogeny; or c) zircon formed in the Superior orogeny and cooled in the Grenville orogeny. The only large

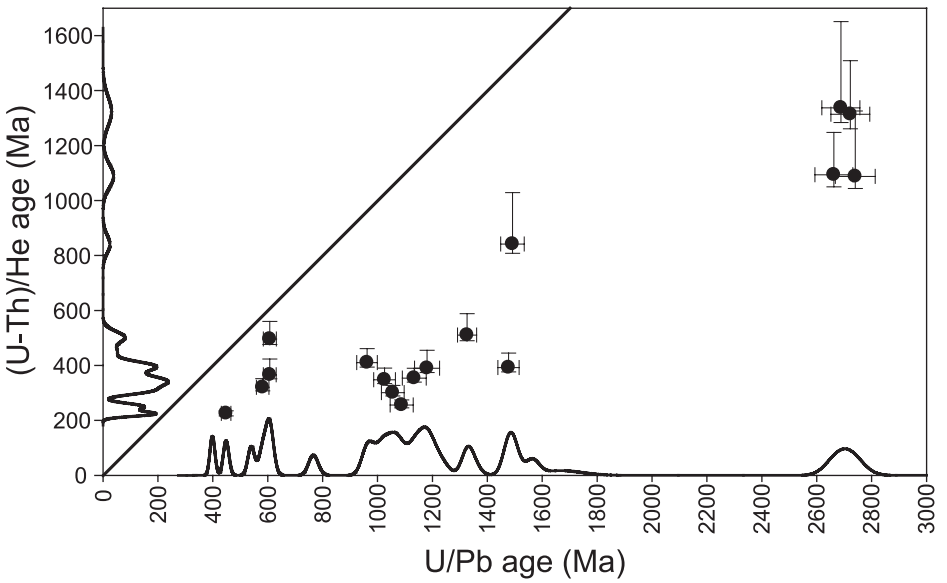

Fig. 6. He-Pb double-dating age distributions from the Navajo sandstone (after Rahl and others, 2003). Probability density plots for U/Pb and He are also shown on horizontal and vertical (respectively) axes. Black line is first-cycle volcanic trend (equal He and U/Pb ages). U/Pb and lower limit (U-Th)/He error bars are 1σ. Upper limit He error bars are ages using standard α-ejection correction instead of detrital approach (eq 6). These upper bound error bars are likely extreme upper limits, because all grains show significant rounding. Most zircons have Grenville U/Pb ages with Appalachian He ages, or Appalachian U/Pb and He ages. These features strongly suggest a source in eastern North America such as the Appalachian/Caledonide orogen. The zircons with Archean U/Pb and Grenvillian He ages may represent sources in the Superior shield that were involved in Grenville-age uplift/exhumation.

region with widespread Grenvillian formation ages and known to have experienced a major, widespread orogenic event in the early-mid Paleozoic (and with widespread early-mid Paleozoic zircon fission-track ages) is the Appalachian-Caledonian orogen of eastern North America. Previous studies have documented that a very large fraction of zircons from this orogen have crystallization ages of ~1.0 to 1.1 Ga, and Paleozoic fission-track ages (for example, Roden and others, 1993; Naeser and others, 2000; Eriksson and others, 2003, 2004). Rahl and others (2003) interpreted this result as evidence for large-scale fluvial transport of detritus from this region to the west in the early Mesozoic, followed by aeolian transport from the north-northwest, to the present location of the Navajo sandstone. A much smaller population of grains appears to be derived from sources with 1.3 to 1.5 Ga U/Pb ages and widely ranging He ages, which may represent contributions from the mid-continent such as exposed in ancestral Rockies uplifts.

The interpretations of Rahl and others (2003) generally concur with another recent U/Pb-dating study of a much larger population of Navajo sandstone zircons, which found similar age distributions in U/Pb ages (Dickinson and Gehrels, 2003). Both of these studies are also in agreement with previous Nd isotopic provenance evidence suggesting that during much of the Mesozoic, the majority of the surface of the North American continent was covered by sediment derived from the Appalachian orogen (Patchett and others, 1999). The advantage of the He-Pb double-dating technique for this application is that it clearly restricted the range of potential source regions for the Navajo sandstone with double dating of fewer than 20 zircons. Knowledge of U/Pb ages of the zircons alone also strongly suggests an Appalachian

source, but requires a larger number of analyses to establish confident provenance resolution because it provides only formation ages. In this case, the combination of Grenvillian formation ages with Appalachian orogen cooling ages provides the strongest indicator of an eastern North American provenance; the other two main populations provide further support.

Another interesting feature of the U/Pb probability density plot is the low abundance of Archaean zircons. Our unpublished U/Pb ages on zircons from a Wisconsin loess shows, as expected, that the dominant peak is at 2.7 Ga. This peak is not well represented in the Mississippi River data (see below), suggesting that loess is not a major contributor to the river's sediment load.

Finally, it is noteworthy that a detrital zircon fission-track study came to a very different provenance interpretation for the Navajo sandstone. Jennison (ms, 1980) found two age peaks of the detrital grain population, at 306 ± 7 and 229 ± 5 Ma, and interpreted these as derived from sources eroded in the Ancestral Rockies and Sonoma orogenies, respectively. Our results also indicate that the cooling ages of most zircons in the Navajo sandstone are 200 to 400 Ma, but the U/Pb dates on most of these same grains are clearly more consistent with a source in the Grenvillian terranes of eastern North America, and effectively limit the Ancestral Rockies or Sonoma orogen to minor, if any, contributions. The lack of crystallization age constraints in Jennison (ms, 1980) ZFT study may be part of the reason for its different conclusion, but another reason may be the fact that Jennison (ms, 1980) found that less than 1 percent of the zircons were dateable by ZFT methods, presumably due to high track densities in these relatively old crystals. Because this effectively limited the dating to young grains and a fraction of the older grains with low U, this underestimated or failed to identify the contribution from zircons with older Appalachian cooling ages (~400 – 500 Ma), and especially the distinctive population with Grenvillian cooling ages.

Mississippi River Delta - Interior Continental Drainage

Sediment of the Mississippi River has received little geochronologic attention. Hurley and others (1961) measured K/Ar ages of silt- and sand-sized fractions of delta sediment, and obtained ages generally between about 200 and 350 Ma, although some samples were as old as 950 Ma, and smaller size fractions tended to yield younger ages, including one as young as 102 Ma. Geologic interpretations from these data are difficult, but Hurley and others discussed the importance of detritus from the western U.S. in the delta. Meyer (ms, 2000) and Meyer and Garver (2000) analyzed fission-track ages of zircon from sediment from both the lower Mississippi near Natchez, Mississippi, and from the delta near Grand Isle, Louisiana. Ninety zircons from the Natchez sample showed a broad distribution of ages between 8 and 580 Ma, and a single age at 1.6 Ga, and 45 grains from the delta sample showed a similarly broad pattern with ages between 28 and 650 Ma, with one age at 1.0 Ga. Neither of the samples showed any obviously separable peaks within the larger age populations, although the Natchez sample could be interpreted as having a slightly higher probability density at ~25 to 30 Ma, and the Grand Isle sample having peaks at ~60 and ~90 Ma.

Figures 7 and 8 show probability densities for 50 U/Pb ages and 17 (U-Th)/He ages, and He-Pb double-date age distributions on zircons from modern sediment of the Mississippi delta near Grand Isle [the same sample analyzed by Meyer and Garver (2000)]. U/Pb ages of 50 grains measured by LA-ICP-MS range from 10 Ma to 1.9 Ga, with the most prominent age peaks at ~30 to 40 Ma, 60 to 110 Ma, 200 Ma, 500 Ma, and 1.0 to 1.2 Ga (fig. 7). A subset of 17 of these grains were also analyzed by zircon He methods (fig. 8). The He ages can be divided into three main groups: group one, with only one grain, has a He age of 850 Ma and U/Pb age of 1.04 Ga. The second group, comprising three crystals, has He ages of 307 to 376 Ma and U/Pb ages of either 0.5 or 1.0 to 1.1 Ga. This combination of ages with either Grenville or Appalachian formation

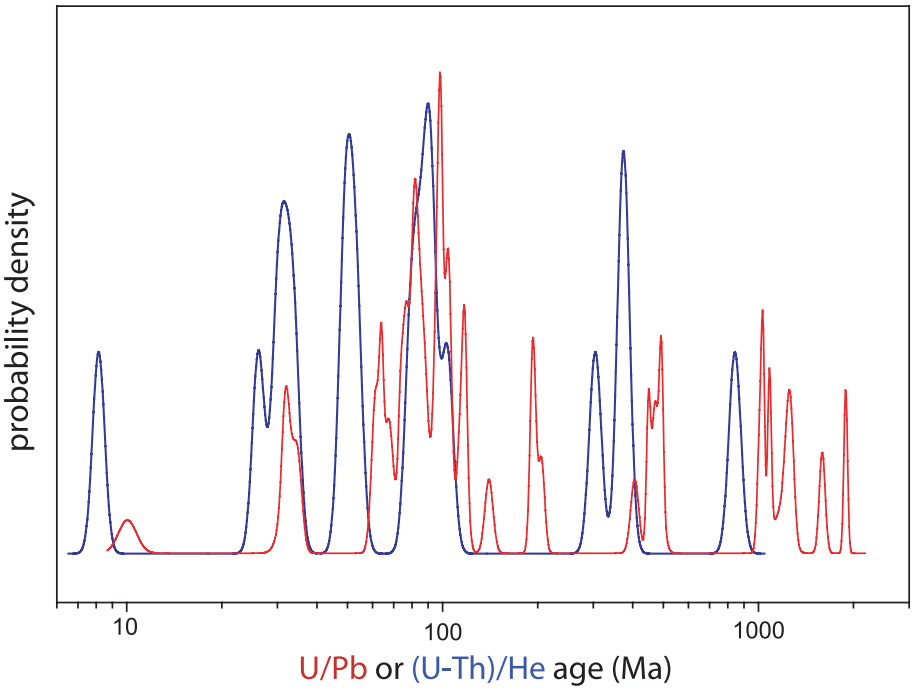

Fig. 7. Probability density plot of zircon U/Pb (red) and (U-Th)/He (blue) ages on Mississippi delta sample NM9906. U/Pb ages range from 10 Ma to 1.9 Ga, with prominent peaks at ~30 to 40 Ma, 60 to 110 Ma, 200 Ma, 500 Ma, and 1.0 to 1.2 Ga. He ages range from 8.2 to 850 Ma, and show peaks at 26 to 34 Ma, 50 to 55 Ma, ~80 to 100 Ma, and 300 to 380 Ma. This and subsequent probability density plots were constructed using the log-scaling procedures described in Brandon (1996).

ages and Appalachian cooling ages, is similar to most of the zircons in the Navajo sandstone, and most likely reflects an Appalachian source.

The last group has U/Pb ages less than 200 Ma, and He ages less than 100 Ma, which almost certainly represents contributions of rivers draining the western U.S. where rocks of this age are found. A remarkable aspect of this group is the abundance of zircons with differences in U/Pb and He ages of less than 10 Myr. Many of the zircons with formation ages less than 110 Ma fall on or very close to the 1:1 trend for He and U/Pb ages, denoting crystals derived from first-cycle volcanic or hypabyssal rocks (fig. 8B). The concordance of He and U/Pb ages for zircons ranging from as young as 10 Ma to as old as 105 Ma is consistent with a large contribution from Cretaceous through Miocene volcanic rocks in the source area of the modern Mississippi, though grains from rapidly extending regions such as magmatically active metamorphic core complexes could also conceivably have such features. Also notable in this group is the concentration of zircons with both He and U/Pb ages between about 30 to 35 Ma. Grains with 30 to 40 Ma U/Pb ages form a distinct peak in the probability density distribution (fig. 7), a cooling age peak also seen in the ZFT ages by Meyer (ms, 2000) and Meyer and Garver (2000), and the double dating shows that these crystals have He and U/Pb ages that are the same within error. We suggest that these zircons represent a large contribution of Oligocene volcanic rocks in the Mississippi drainage, which may be derived from easily eroded volcanic-rich Oligocene strata in intermontane basins and the Great Plains (for example, Clark and others, 1967). Oligocene strata in the Great Plains are, in general, considerably richer in volcanic ash than older or younger units (Frazier and Schwimmer, 1987).

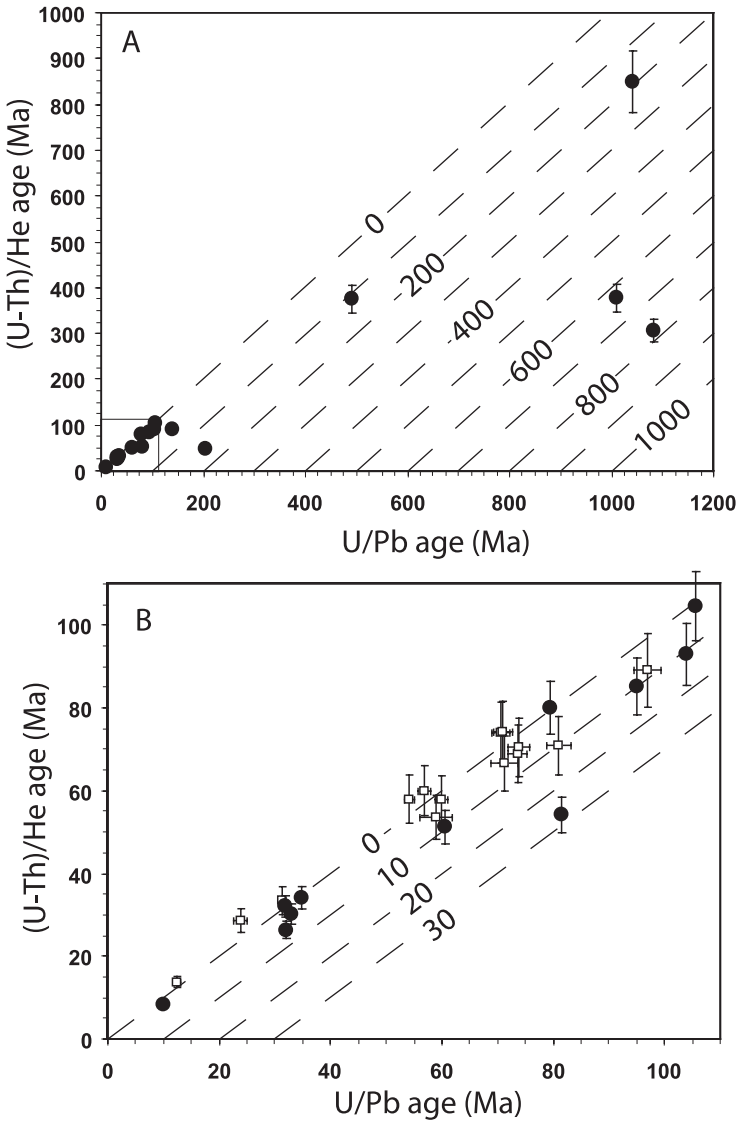

Fig. 8. He-Pb age distributions for the Mississippi delta sample. Dashed lines are contours of He-Pb "lag-time" (the U/Pb-He age difference). Panel B is close-up of small box near origin in panel A. This sample contains a large proportion of zircons with U/Pb ages less than 120 Ma; many of these have He ages that are the same as the U/Pb ages, suggesting derivation from volcanic rocks. Others have relatively short lag-times, also implying near-surface formation. The cluster of zircons with similar He and U/Pb ages at ~35 Ma may be derived from easily-eroded Oligocene volcanic rocks in the Great Plains or intermontane basins of the western U.S. Small open square symbols in panel B are He-Pb double-dates of zircons from the Missouri River (only grains younger than 110 Ma are shown), from unpublished data of Reiners and others.

A large proportion of the western drainage of the Mississippi river is carried by the Missouri River. Figure 8B also shows He-Pb double-dates on detrital zircons younger than 110 Ma from the Missouri, at its confluence with the Mississippi in St. Louis (Reiners and others, unpublished data). Many of the Missouri River zircons also have indistinguishable He and U/Pb ages, although the Missouri population contains fewer

Oligocene grains and many more early Paleogene (50 – 60 Ma) and Late Cretaceous (70 – 80 Ma) zircons that may be derived from rapidly exhumed crustal domains (for example, Foster and Fanning, 1997) or magmatism associated with Idaho and Boulder batholiths in Idaho and Montana (for example, Hamilton and Myers, 1974; Armstrong and others, 1977). This may mean that a large proportion of the Oligocene zircons in the Mississippi are derived from other, more southerly rivers in the western U.S., such as the Arkansas or Canadian rivers. These rivers are closer to the voluminous Oligocene volcanic rocks in Colorado and New Mexico (Lipman and others, 1970; Steven, 1975; Lipman and others, 1978) most of whose modern drainages now flow to the west, however.

Although U/Pb ages of the Mississippi delta zircons alone could have constrained the source of most of the Mississippi detritus to the western U.S. because of the paucity of such young rocks in the east, the combined He-Pb ages of these samples provide the additional constraint that most of this material is from volcanic or hypabyssal rocks, not deeply eroded orogenic roots. The abundance of volcanic or hypabyssal zircons in the Mississippi river delta, thousands of kilometers from any significant volcanic rocks younger than Jurassic, is also somewhat surprising because such grains appear to be relatively rare in active margin sediments, as discussed in the next two examples.

Finally, discussion of the significance of these detrital signals in Mississippi River sediments should acknowledge the potential importance of temporal changes in sediment provenance over relatively short time-scales. For example, changes in local erosion and sediment delivery patterns caused by glacial-interglacial cycles, modern land-use changes, or even storm events could potentially change detrital delivery patterns over short timescales that may be seen in He-Pb age spectra among sediments with age differences on yr-kyr timescales. On longer timescales, fluvial network changes may be discernable in He-Pb detrital records. If, for example, prior to continental glaciation the Missouri River drained north to Hudson Bay rather than the modern route south into the Mississippi, then pre- or early-Pliocene Mississippi sediments should show a much smaller population of volcanic and pre-100-Ma zircons from the western U.S.

Paleoriver Channels, Northeastern Oregon

In the Elkhorn and Wallowa Mountains of northeastern Oregon, unusual paleofluvial deposits have been found in several locations at relatively high elevation. The deposits have long been recognized as potentially important for paleotopographic and paleogeographic reconstructions (Stearns, 1954; Taubeneck, 1955; Allen, 1991; Cisneros, 1999; Trafton, 1999), but their ages and provenance are poorly understood. The deposits lie above an unconformity between underlying, generally plutonic, rocks of Mesozoic accreted terranes, and overlying Tertiary volcanic rocks, either Miocene flood basalts of the Columbia River Basalt Group or Oligocene intermediate to silicic volcanic rocks. The paleofluvial deposits comprise sand, gravel and boulders up to 75 cm in diameter, with paleoflow directions to the northwest. The clasts are dominantly quartzite, chert, and porphyritic volcanic rocks, and are similar to rocks now located tens to hundreds of kilometers to the east, in the Belt Supergroup, miogeoclinal Paleozoic strata, and early Tertiary volcanic rocks of central Idaho and western Montana. We sampled sand-sized fractions of these deposits in two areas, Camp Carson and French Diggings, in the Elkhorn mountains, with the goal of using He-Pb zircon double dating to constrain both the depositional ages and provenance of these fluvial sediments.

Figure 9 shows the probability density distribution of 109 U/Pb ages and 23 (U-Th)/He ages for zircons from all three samples. There is little difference in either He or U/Pb age distributions among the samples. Most crystals have U/Pb ages at ~70 to 90 Ma and He ages at ~40 to 60 Ma. There are also smaller U/Pb age peaks between

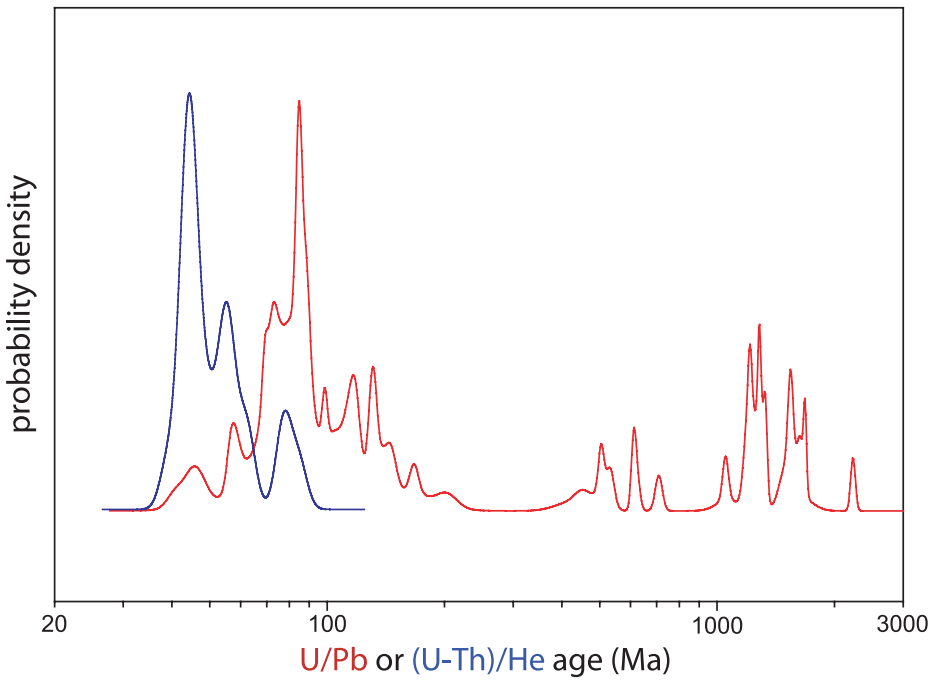

Fig. 9. Probability density plot of zircon U/Pb and (U-Th)/He ages for three samples from paleofluvial channel deposits currently exposed at high elevation in the Elkhorn Mountains of northeastern Oregon. There is little difference in either He or U/Pb age distributions among the samples. The largest peak of U/Pb ages is at ~70 to 90 Ma. All samples also have smaller peaks between ~120 to 140 Ma, and there is a significant population at 1.4 to 1.7 Ga. Two of the samples also contain a few zircons with ages as young as 41 to 48 Ma, providing a maximum age constraint for the deposits. The He ages show a much more restricted range of ages, with the largest peak at 40 to 50 Ma, a second at ~50 to 65 Ma, and a third at 70 to 90 Ma.

~120 to 150 Ma, and there is a significant population in a characteristic 1.4 to 1.7 Ga age range. Two of the samples also contain a few zircons with U/Pb ages as young as 41 to 48 Ma, providing a maximum depositional age constraint for the deposits.

The combined U/Pb and He ages on single grains (fig. 10) provide a more robust constraint on the maximum age of the deposit, by showing that the two zircons with the youngest U/Pb ages (41 ± 3 and 46 ± 4 Ma, 2σ) have He ages that are indistinguishable (42 ± 3 and 50 ± 4 Ma, respectively) from the U/Pb ages. This finding suggests that these youngest grains, with concordant U/Pb and He ages, are first-cycle volcanic zircons. Although this still only provides a maximum age constraint for the deposit, the identification of the youngest grains as first-cycle volcanic raises the likelihood that their age is close to the depositional age. This approach is similar to using ages of zircons from tephra layers interbedded with sediments for depositional age constraints, and assuming that the zircons are first-cycle volcanic with zero-age lag-times. At least in settings where volcanic rocks contribute to sediments, the He-Pb double-dating method can essentially identify dispersed tephra in regular clastic sediments.

A somewhat surprising observation of the He-Pb double-date distribution is that the He ages are ~40 to 50 Ma not only for first-cycle zircons with similar U/Pb ages, but also for zircons with much older U/Pb ages, including most of those with Cretaceous, Cambrian, and Paleoproterozoic U/Pb ages. Remarkably, the zircon with the oldest U/Pb age in this suite, 2.23 ± 0.02 Ga, also has a He age of 48.6 ± 3.9 Ma, indistinguishable from the youngest He ages. Holding a zircon with the U concentra-

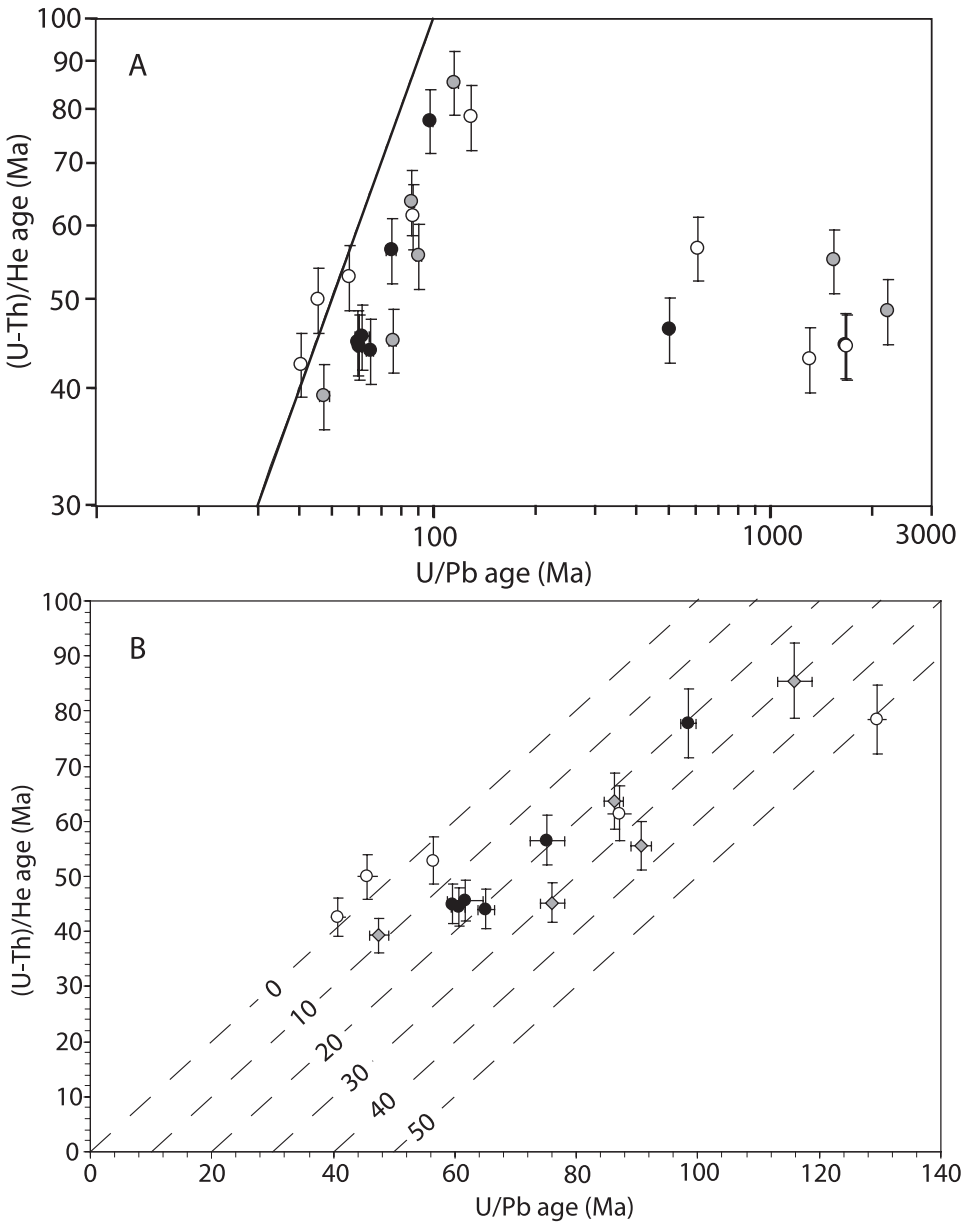

Fig. 10. He-Pb age distributions for the Elkhorn Mountains paleofluvial channel deposits. Black circles are from sample FD-1 (French Diggings 1), gray circles from FD-2 (French Diggings 2), and white circles from CAR-1 (Camp Carson). See table 2 for details. The two zircons with the youngest U/Pb ages (41 ± 3 and 46 ± 4 Ma, errors at 2σ) have indistinguishable He ages (42 ± 3 and 50 ± 4 Ma, respectively), identifying them as first-cycle volcanic zircons, and providing a maximum age constraint for the deposit. Despite U/Pb ages ranging from 40 Ma to 2.2 Ga, the vast majority of zircons have He ages ranging from 40 to 55 Ma, implying a widespread thermal event such as plutonism and/or exhumation at this time in the source regions to the east.

tion of this crystal (340 ppm; table 2) at low temperatures for 2.2 byr could potentially lead to accumulated radiation damage of ~3.4 x 10^{18} α/g, beyond the critical threshold for radiation damage effects on He diffusion. However we consider it

unlikely that the He diffusion properties of this zircon were significantly affected by radiation damage, primarily because the concordance of the 49-Ma age with others seems an improbable coincidence.

The abundance of zircons with 40 to 50 Ma He ages and widely varying U/Pb ages could be explained by three possibilities: 1) these zircons could be derived from 40 to 50-Ma volcanic rocks containing large proportions of inherited zircons (although in this case we would have expected to observe abundant young rims in the U/Pb dating); 2) they could be plutonic zircons or recycled sedimentary zircons that were exhumed through the ~180 °C closure depth at 40 to 50 Ma; 3) they could be from a wide variety of rock types that were reheated and reset by a large-scale thermal event at 40 to 50 Ma, such as widespread shallow plutonism. These explanations need not be mutually exclusive and in fact would be likely to be associated in space and time. Eocene "Challis" volcanism was widespread and voluminous throughout modern Idaho, Montana, and other regions between 40 to 50 Ma (for example, Armstrong, 1974; Brandon and Vance, 1992; Janecke and Snee, 1993), though the abundance of inherited zircons in the Challis volcanic rocks is not known. Most of the low-angle normal faulting exhumation in the Bitteroot Mountains is thought to have occurred between 55 to 40 Ma (for example, Foster and others, 2001), at least in northern Idaho, which could have exhumed and cooled large quantities of zircon from crustal depths greater than ~5 to 9 km. Sweetkind and Blackwell (1989) also found abundant 40 to 50 Ma zircon fission-track ages in the Idaho batholith and, together with other evidence, inferred rapid cooling through about 150 °C at this time. And finally, the Challis magmatic events associated with volcanism may have raised geothermal gradients over a large area, producing a widespread thermal anomaly that reset zircons to depths of only a few kilometers (compared with ~7 – 8 km in crust with more typical geothermal gradients).

Another somewhat surprising observation of the He-Pb age distribution is that although there is a population of Early and Middle Proterozoic zircons in these samples, the zircons with He ages greater than 57 Ma all have U/Pb ages younger than 130 Ma. Within this group of zircons with 41 to 130 Ma U/Pb ages, there is a weak correlation between U/Pb and He age. Crystals with U/Pb ages as old as ~65 Ma all have He ages that are essentially indistinguishable from the 40 to 50 Ma He age range, but crystals with U/Pb ages older than this generally have older He ages, including the three oldest He ages between 78 and 86 Ma (and corresponding U/Pb ages of 98 – 130 Ma). Interestingly, these oldest He ages fall within the largest peak of the U/Pb age population: 70 to 90 Ma, which must represent large amounts of crustal melting and crystallization of new zircons, probably associated with intrusion of older phases of the Idaho Batholith (for example, Armstrong and others, 1977; Toth and Stacey, 1992). It is noteworthy however, that the thermal effects of this event, which could be either related to either reheating or exhumation caused by the batholith, appear to only be evident in zircons with older formation (U/Pb) ages. In other words, it appears that although most of the U/Pb ages record formation of the 70 to 90-Ma parts of the Idaho batholith, few of the He ages do, and those that do are derived from slightly older rocks. These units may have been the roof or wallrocks to the batholith, which have now been stripped away to expose the batholithic rocks. Most of this exhumation responsible for the exposure of the Idaho batholithic rocks evidently occurred in Challis time, as most of the zircons with 70 to 90 Ma formation ages have 40 to 50 Ma He ages (also see Sweetkind and Blackwell, 1989; Foster and others, 2001).

The results of the paleofluvial studies and their implications for crustal formation and thermal histories are similar in some ways to those of the Appalachians recorded in the Navajo sandstone. In the Navajo population, two major orogenic or crustal formation events (Grenville and Appalachian) are evident in three separate groups of

TABLE 2

(U-Th)/He and U/Pb data for double-dated zircons

Fish Canyon Tuff

sample name	(U-Th)/He data Ft	corr age (Ma)	± (2σ) (Ma)	half-width (μm)	mass (ug)	U (ppm)	Th (ppm)	Th/U	LA-ICP-MS U/Pb data U (ppm)	Th (ppm)	age (Ma)	± (2σ) (Ma)	Th/U
ANUFCT21	0.742	28.2	2.3	38	3.8	459	194	0.42	401	193	28.5	0.46	0.48
ANUFCT23	0.696	25.5	2.0	33	2.1	391	192	0.49	408	219	28.9	0.50	0.54
ANUFCT24	0.747	28.8	2.3	48	4.4	422	191	0.45	353	167	29.3	0.50	0.47
ANUFCT25	0.769	29.4	2.4	44	5.1	389	154	0.40	454	260	28.2	0.54	0.57
ANUFCT35	0.717	28.5	2.3	35	2.7	403	200	0.50	447	207	28.4	0.52	0.46
ANUFCT26	0.730	30.2	2.4	33	3.1	396	249	0.63	312	208	28.9	0.70	0.67
ANUFCT27	0.775	28.4	2.3	44	5.7	424	219	0.52	520	391	31.2	1.16	0.75
ANUFCT32	0.717	27.2	2.2	39	2.3	500	272	0.54	1029	546	28.4	0.40	0.53
ANUFCT33	0.697	29.5	2.4	32	2.3	355	190	0.54	553	312	27.3	1.90	0.56
ANUFCT34	0.715	29.8	2.4	35	2.6	341	220	0.65	477	256	27.8	0.90	0.54
ANUFCT36	0.650	30.6	2.4	29	1.6	442	282	0.64	503	328	29.0	1.48	0.65
ANUFCT38	0.672	27.6	2.2	30	1.7	404	249	0.61	418	233	27.5	0.56	0.56
ANUFCT5Nb	0.790	28.8	2.3	47	7.3	446	229	0.51	456	204	29.2	0.48	0.45
ANUFCT6Nb	0.812	29.5	2.4	54	10.8	474	245	0.52	482	243	29.9	0.50	0.50
ANUFCT40Nb	0.731	30.5	2.4	37	3.2	347	179	0.51	361	148	29.1	0.98	0.41
FCTANU7	0.828	26.2	2.1	54	15.4	245	136	0.55	475	206	29.5	0.52	0.43
FCTANU3	0.750	28.6	2.3	41	4.0	332	211	0.63	315	154	28.9	0.64	0.49
ANUFCT28	0.715	27.8	2.2	34	2.9	368	196	0.53	400	241	28.4	0.86	0.60
FCTANU8	0.817	28.2	2.3	57	1.4	277	155	0.56	379	124	29.0	0.56	0.33
average		28.6									28.8		
2 stdev		2.7									1.8		
% 2 stdev		9.4									6.3		

TABLE 2
(continued)

Mississippi delta sample NM9906

sample name	(U-Th)/He data								LA-ICP-MS U/Pb data				
	Ft	corr age (Ma)	± (2σ) (Ma)	half-width (μm)	mass (ug)	U (ppm)	Th (ppm)	Th/U	U (ppm)	Th (ppm)	age (Ma)	± (2σ) (Ma)	Th/U
NM9906-1	0.681	30.2	2.4	29	2.3	301	241	0.80	159	143	33.0	0.88	0.90
NM9906-4	0.705	8.2	0.7	30	4.1	271	142	0.52	192	104	10.1	0.44	0.54
NM9906-5	0.714	54.0	4.3	46	2.4	208	76	0.36	66	39	81.6	1.94	0.59
NM9906-13	0.716	85.0	6.8	39	2.8	334	176	0.53	263	158	95.1	1.52	0.60
NM9906-14	0.676	49.0	3.9	33	2.5	191	2662	13.96	127	59	205.6	3.20	0.47
NM9906-20	0.660	92.8	7.4	27	1.7	615	223	0.36	302	115	103.9	1.40	0.38
NM9906-24	0.738	51.1	4.1	32	4.2	203	87	0.43	150	43	60.5	1.12	0.29
NM9906-15	0.663	34.1	2.7	27	2.0	381	172	0.45	309	124	34.9	0.70	0.40
NM9906-25	0.649	104.3	8.3	27	1.5	367	167	0.45	309	157	105.6	1.40	0.51
NM9906-29	0.631	376.3	30.1	27	1.0	165	103	0.62	96	66	492.7	4.72	0.69
NM9906-39	0.659	32.0	2.6	30	1.3	360	219	0.61	346	200	31.8	0.54	0.58
NM9906-42	0.716	91.0	7.3	34	2.8	92	41	0.44	55	13	140.2	2.78	0.24
NM9906-12	0.644	849.8	68.0	25	1.9	288	218	0.76	154	97	1043	8.60	0.63
NM9906-45	0.698	378.0	30.2	29	3.3	147	41	0.28	183	63	1011	12.40	0.34
NM9906-48	0.743	307.1	24.6	40	3.5	292	81	0.28	284	69	1084	9.40	0.24
NM9906-43	0.638	26.3	2.4	25	2.0	142	136	0.96	124	128	32.0	1.20	1.03
NM9906-44	0.692	79.9	7.2	32	2.7	114	44	0.39	91	44	79.4	1.80	0.48

TABLE 2
(continued)

Northeastern Oregon Paleofluvial Deposits

sample name	(U-Th)/He data Ft	corr age (Ma)	± (2σ) (Ma)	half-width (μm)	mass (ug)	U (ppm)	Th (ppm)	Th/U	LA-ICP-MS U/Pb data U (ppm)	Th (ppm)	age (Ma)	± (2σ) (Ma)	Th/U
CAR1	0.787	43.2	3.5	46	8.6	634	989	1.56	276	136	1309	17.20	0.49
CAR2	0.767	56.8	4.5	40	6.6	379	188	0.50	231	144	610.6	5.60	0.62
CAR4	0.800	52.8	4.2	48	10.3	336	148	0.44	625	267	56.5	0.80	0.43
CAR11	0.838	78.5	6.3	66	14.8	322	149	0.46	630	364	129.5	1.40	0.58
CAR17	0.801	49.9	4.0	50	8.9	390	166	0.42	336	139	45.6	1.60	0.41
CAR18	0.741	61.4	4.9	34	6.3	425	158	0.37	280	82	87.1	1.80	0.29
CAR28	0.818	44.5	3.6	58	8.2	386	68	0.18	448	133	1681	10.00	0.30
CAR34	0.885	42.6	3.4	95	45.4	522	257	0.49	912	447	40.8	1.20	0.49
FD2-1	0.735	63.7	5.1	35	4.4	346	81	0.23	194	61	86.2	1.60	0.32
FD2-6	0.782	55.6	4.4	43	7.7	517	170	0.33	449	187	90.7	1.60	0.42
FD2-7	0.823	45.2	3.6	56	16.0	158	29	0.18	102	46	76.0	2.00	0.45
FD2-16	0.757	39.3	3.1	42	4.4	399	170	0.43	160	154	47.5	1.60	0.97
FD2-23	0.790	55.0	4.4	51	7.1	1345	370	0.28	350	165	1540	16.60	0.47
FD2-30	0.926**	85.5	6.8	71	23.1	353	139	0.39	115	51	115.9	2.80	0.45
FD2-35	0.802	48.6	3.9	51	8.6	340	94	0.28	241	94	2231	20.60	0.39
FD1-3	0.872	44.6	3.6	83	32.1	152	67	0.44	109	19	1674	33.20	0.17
FD1-11	0.865	44.1	3.5	83	24.3	352	20	0.06	617	55	65.1	1.40	0.09
FD1-15	0.865	45.0	3.6	79	26.4	1363	274	0.20	1559	420	59.7	0.60	0.27
FD1-17	0.868	45.6	3.6	82	28.0	78	22	0.28	130	45	61.7	3.00	0.34
FD1-18	0.846	44.4	3.6	66	22.4	352	91	0.26	668	237	60.6	1.20	0.35
FD1-19	0.866	77.8	6.2	74	32.1	1030	136	0.13	758	109	98.5	1.20	0.14
FD1-25	0.879	46.4	3.7	92	41.2	582	271	0.46	258	59	502.8	5.40	0.23
FD1-35	0.801	56.5	4.5	47	11.6	105	51	0.49	152	75	75.2	2.80	0.49

Note: **Zonation-corrected F_T, based on laser-ablation depth profiling (Hourigan and others, 2005).

TABLE 2
(continued)

Coastal Olympic Subduction Complex sample 162

	(U-Th)/He data								LA-ICP-MS U/Pb data				
sample name	Ft	corr age (Ma)	± (2σ) (Ma)	half-width (μm)	mass (ug)	U (ppm)	Th (ppm)	Th/U	U (ppm)	Th (ppm)	age (Ma)	± (2σ) (Ma)	Th/U
OZ162-1	0.860	24.1	1.9	82	21.1	112	23	0.20	163	37	91.4	1.17	0.23
OZ162-2	0.863	18.2	1.5	84	22.2	110	36	0.33	95	26	85.2	1.66	0.27
OZ162-3	0.875	27.8	2.2	87	36.1	216	67	0.31	192	104	82.9	1.28	0.54
OZ162-4	0.846	13.5	1.1	67	19.5	274	153	0.56	350	192	18.4	1.12	0.55
OZ162-5	0.838	30.9	2.5	64	15.6	297	75	0.25	192	50	145.0	2.13	0.26
OZ162-6	0.860	20.0	1.6	74	25.1	158	36	0.23	154	26	95.9	3.08	0.17
OZ162-7	0.855	13.7	1.1	72	23.7	117	48	0.41	159	67	23.8	1.06	0.43
OZ162-8	0.858	59.4	4.7	76	26.6	221	72	0.33	194	49	131.2	2.10	0.25
OZ162-9	0.870	22.1	1.8	77	35.9	114	54	0.47	120	56	84.9	1.76	0.46
OZ162-10	0.858	16.3	1.3	79	20.5	163	41	0.25	107	47	68.4	1.53	0.44
OZ162-11	0.865	32.1	2.6	74	16.2	241	61	0.25	645	33	80.4	1.17	0.05
OZ162-12	0.841	24.1	1.9	65	16.4	117	31	0.27	134	26	82.8	1.79	0.19
OZ162-13	0.846	22.6	1.8	69	17.3	161	66	0.41	239	54	84.2	1.24	0.23
OZ162-15	0.823	14.7	1.2	60	10.9	321	87	0.27	218	40	87.4	2.23	0.19
OZ162-16	0.808	12.9	1.0	55	8.4	251	84	0.33	347	96	17.0	0.59	0.28
OZ162-17	0.845	52.8	4.2	70	16.2	158	69	0.44	58	14	126.2	3.20	0.24
OZ162-19	0.836	29.9	2.4	65	14.4	159	57	0.36	114	33	91.0	2.17	0.29
OZ162-20	0.865	19.1	1.5	78	26.5	60	19	0.32	87	20	88.0	2.11	0.23
OZ162-21	0.843	20.3	1.6	67	16.3	319	64	0.20	318	69	101.8	2.32	0.22
OZ162-25	0.823	26.2	2.1	63	10.7	823	273	0.33	615	166	107.7	4.13	0.27
OZ162-26	0.863	34.4	2.8	81	24.5	300	84	0.28	109	26	128.4	2.78	0.24

TABLE 2
(continued)

sample name	(U-Th)/He data Ft	corr age (Ma)	± (2σ) (Ma)	half-width (μm)	mass (ug)	U (ppm)	Th (ppm)	Th/U	LA-ICP-MS U/Pb data U (ppm)	Th (ppm)	age (Ma)	± (2σ) (Ma)	Th/U
Coastal Olympic Subduction Complex sample 211													
OZ211-1	0.869	39.1	3.1	79	21.1	134	36	0.27	184	54	83.3	1.60	0.29
OZ211-2	0.886	45.4	3.6	90	34.3	165	53	0.32	82	36	151.6	2.80	0.44
OZ211-5	0.897	12.6	1.0	100	45.3	212	66	0.31	282	69	14.2	0.40	0.24
OZ211-6	0.860	13.5	1.1	77	15.9	341	110	0.32	257	88	14.4	0.80	0.34
OZ211-10	0.873	13.0	1.0	85	21.4	200	63	0.32	143	43	16.4	0.80	0.30
OZ211-11	0.881	11.9	1.0	94	25.2	213	67	0.31	237	55	14.3	0.60	0.23
OZ211-13	0.905	13.8	1.1	112	53.8	173	54	0.32	159	56	14.7	0.60	0.35
OZ211-18	0.860	12.3	1.0	74	17.4	388	199	0.51	238	49	15.2	0.80	0.20
OZ211-28	0.889	13.7	1.1	100	32.0	232	68	0.29	455	124	15.5	0.40	0.27
Ukelayet flysch sample 95JG-16													
95JG-16-3	0.710	38.8	3.1	34	2.5	659	325	0.49	411	173	50.3	0.76	0.42
95JG16-4	0.763	63.0	5.0	43	4.5	308	83	0.27	313	31	2070	45.60	0.10
95JG-16-7	0.700	40.4	3.2	33	2.2	412	294	0.71	418	332	66.1	1.08	0.79
95JG16-11	0.742	42.5	3.4	41	3.5	60	51	0.84	54	33	1772	29.20	0.62
95JG-16-12	0.708	56.1	4.5	36	2.3	159	165	1.04	192	149	123.0	1.28	0.78
95JG-16-14	0.717	33.9	2.7	34	2.8	203	75	0.37	122	40	114.0	1.62	0.32
95JG16-15	0.675	37.3	3.0	29	1.9	430	148	0.34	215	46	56.8	1.26	0.21
95JG16-18	0.732	44.0	3.5	38	3.3	504	341	0.68	442	325	126.4	1.70	0.74
95JG16-19	0.719	38.4	3.1	34	3.2	115	59	0.52	62	23	90.2	2.08	0.36
95JG16-24	0.696	40.7	3.3	32	2.4	147	110	0.75	144	98	271.2	4.80	0.68
95JG16-10	0.748	27.4	2.2	41	3.7	615	329	0.54	908	422	79.7	1.84	0.46
95JG16-23	0.722	34.0	2.7	38	2.6	167	112	0.67	91	38	61.3	1.58	0.42
95JG16-25	0.687	27.8	2.2	34	1.7	104	64	0.62	90	53	54.0	1.66	0.59
95JG16-26	0.719	71.7	5.7	38	2.5	290	110	0.38	257	98	1705	19.88	0.38
95JG16-28	0.674	45.0	3.6	30	2.3	270	255	0.97	394	301	145.8	2.28	0.76
95JG16-30	0.723	34.4	2.8	35	4.1	170	98	0.59	467	301	109.2	1.34	0.65

TABLE 2
(continued)

Ukelayet flysch sample 95JG-29													
	(U-Th)/He data								LA-ICP-MS U/Pb data				
sample name	Ft	corr age (Ma)	± (2σ) (Ma)	half-width (μm)	mass (ug)	U (ppm)	Th (ppm)	Th/U	U (ppm)	Th (ppm)	age (Ma)	± (2σ) (Ma)	Th/U
95JG-29-16	0.723	31.4	2.5	40	2.5	131	107	0.81	96	84	164.5	2.44	0.87
95JG-29-18	0.712	36.0	2.9	35	2.4	81	42	0.52	72	30	91.6	2.20	0.42
95JG-29-20	0.732	59.2	4.7	40	3.0	140	91	0.65	74	52	372.6	4.96	0.70
95JG-29-21	0.720	39.6	3.2	36	2.6	318	122	0.38	311	112	209.6	2.02	0.36
95JG29-11	0.783	38.8	3.1	48	6.2	93	64	0.69	101	101	319.1	5.80	0.99
95JG29-13	0.754	78.5	6.3	32	4.7	704	259	0.37	654	297	526.9	6.16	0.45
95JG29-26	0.729	39.4	3.2	39	2.8	66	42	0.63	69	50	356.3	5.48	0.73
95JG29-30	0.728	41.4	3.3	35	3.4	592	220	0.37	564	215	99.0	1.14	0.38
95JG29-33	0.737	48.5	3.9	39	3.1	341	184	0.54	316	197	328.2	8.60	0.62
95JG29-36	0.768	49.3	3.9	46	3.2	487	45	0.09	395	62	1981	30.80	0.16
95JG29-15	0.710	35.9	2.9	32	2.8	377	103	0.27	536	128	140.2	1.90	0.24
95JG29-17	0.714	32.4	2.6	37	2.3	273	161	0.59	174	78	73.1	4.58	0.45
95JG29-23	0.717	38.1	3.0	36	2.6	182	136	0.75	164	93	90.0	1.62	0.57
95JG29-31	0.737	29.5	2.4	38	3.7	74	45	0.61	56	27	50.6	2.24	0.49
95JG29-39	0.738	56.1	4.5	37	4.7	354	124	0.36	414	157	198.1	3.12	0.38

crystals with distinctive age combinations: 1) Archean formation ages with Grenvillian cooling ages, 2) Grenvillian formation ages with Appalachian cooling ages, and 3) Appalachian formation ages with Appalachian cooling ages. In the Oregon paleofluvial sediments, two major orogenic or crustal formation events can also be identified, in four major age-combination groups: 1) Paleozoic and Precambrian formation ages with Challis cooling ages, 2) Early to Middle Cretaceous formation ages with early Idaho batholith cooling ages, 3) early Idaho batholith formation ages with Challis cooling ages, and 4) Challis formation ages with Challis cooling ages. The major apparent difference between the Navajo and Oregon cases is that in the Appalachians the oldest formation ages are associated with the oldest cooling ages (Archean and Grenville, respectively), whereas in the Oregon case the oldest formation ages are associated with some of the youngest cooling ages (1.4 – 2.2 Ga, and 40 – 50 Ma, respectively). Evidently, the Challis magmatic- and/or exhumation-related thermal events in this region were widespread and affected rocks of very different ages, whereas in the Appalachians, the youngest event seems to have affected essentially only crust formed in or after Grenville time.

Olympic Subduction Complex, Washington – Active Margin Turbidites

The Olympic Mountains are the emergent forearc accretionary wedge of the Cascadia subduction zone. The Hoh Formation, part of the Olympic Subduction Complex (OSC), is a sequence of Miocene shelf and trench sedimentary rocks that composes a large part of the western Olympic Peninsula (Stewart and Brandon, 2004). We used two samples (211 and 162) from the OSC provided by R. Stewart, in an attempt to constrain the provenance of its zircons, the formation and thermal history of their sources, and to constrain the depositional age of the host rocks. Both samples are coarse sandstones stratigraphically adjacent to layers with benthic foraminifera suggesting ages between about 11.2 and 16.4 Ma. Previous ZFT work by Stewart and Brandon (2004) suggests maximum depositional ages of these units (from minimum ZFT ages) are between 11 and 18 Ma. Sample 162 yielded a minimum ZFT age of $18.3^{+3.3}_{-2.8}$ Ma, and stratigraphic and structural considerations suggest that sample 211 should be younger than this.

Post-depositional thermal histories of these samples can be constrained by zircon and apatite fission-track data from nearby samples, which suggest no resetting of the ZFT system, and partial or mixed resetting (the latter corresponding to apatites with mixed inferred annealing properties) of the AFT system (Brandon and others, 1998; Stewart and Brandon, 2004). Vitrinite reflectance values of samples within about 5 km of these samples range from 0.6 to 2.0 (Snavely and Kvenvolden, 1989). The partial to mixed resetting AFT ages and vitrinite data suggest maximum temperatures of about 120 to 160 °C for likely burial and exhumation histories for these samples, but this is not well constrained by the available data.

Figure 11 shows probability density distributions of 63 U/Pb ages and 30 (U-Th)/He ages for the OSC samples. The youngest U/Pb zircon ages in samples 162 and 211 are 17.0 ± 0.59 Ma and 14.2 ± 0.44 Ma (2σ), respectively, and the oldest U/Pb zircon ages are 145 ± 2.2 Ma and 152 ± 2.8 Ma, respectively. The youngest crystals form a distinctive peak in the U/Pb probability density plot. Another clearly distinctive population has U/Pb ages between 80 to 100 Ma, similar to but slightly older than the main U/Pb age peak in the Oregon paleofluvial deposits. Subsidiary peaks appear in both samples at ~55 Ma, ~70 Ma, and ~125 to 150 Ma. Another noteworthy feature of the U/Pb ages is the paucity of crystals in certain age ranges, most notably between ~20 to 60 Ma, anything older than 140 Ma, and to a lesser degree, between ~110 to 120 Ma. (U-Th)/He ages show a very different probability density distribution than the U/Pb ages, with maxima between ~12 to 14 Ma and ~18 to 35 Ma.

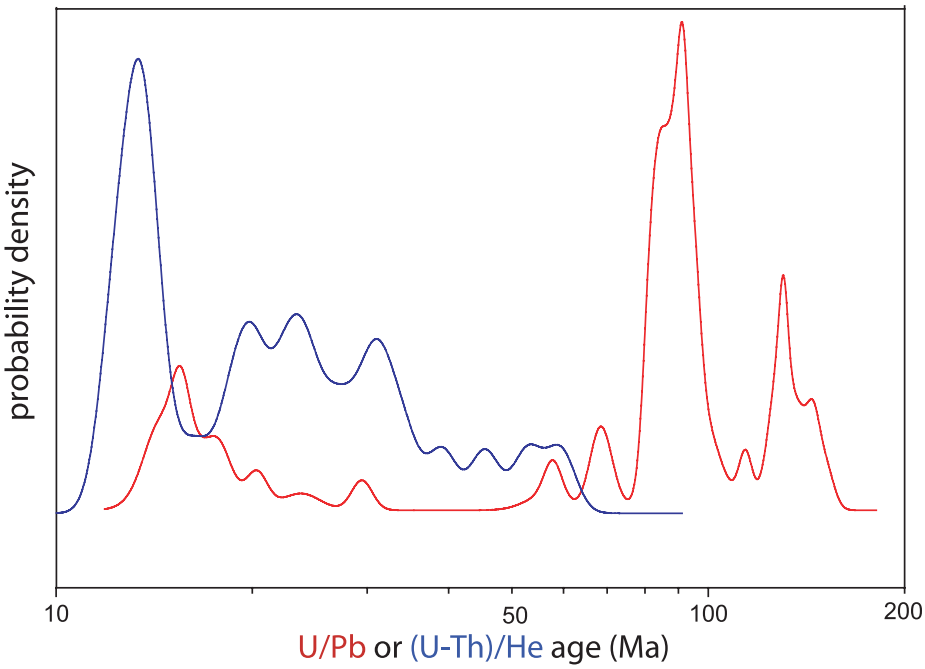

Fig. 11. Probability density plot of zircon U/Pb and (U-Th)/He ages for two samples from the Olympic Subduction Complex [f.k.a. Hoh Formation; Stewart and Brandon (2004)]. These samples have very similar age distributions; samples OZ162 and OZ211 have minimum U/Pb ages of 17.0 ± 0.6 Ma and 14.2 ± 0.44 Ma (2σ), respectively, and maximum ages of 145 ± 2.2 Ma and 152 ± 2.8 Ma, respectively. The most distinctive peaks in both of these samples comprise grains with ages between 80 to 100 Ma, with a subsidiary older peak between ~120 to 140 Ma, and a young peak at ~15 to 18 Ma. A noteworthy feature of the U/Pb ages is the paucity of crystals with ages between ~20 to 60 Ma, or older than 140 Ma. Most He ages occupy the age range least populated by U/Pb ages: ~20 to 60 Ma. The large peak of ~12 to 16 Ma He ages is not statistically representative of its abundance in the sample, as we preferentially selected zircons with the youngest U/Pb ages for He dating, to test for their volcanic origin.

The lack of zircons with early to middle Tertiary U/Pb ages in these rocks is somewhat surprising, given the proximity of the Olympics to the Cascades arc, which has been active since about 40 Ma, and the fact that Oligocene volcanic rocks cover a large part of the modern Washington Cascades. Two possible reasons for this are that the Cascades produce little zircon—either in general, or of the size we would sample in these rocks—or that most of the Olympics sediment was derived not from the magmatic arc, but from the interior northwest, or Coast Mountains to the north. These regions experienced large-scale extension in the Eocene, possibly involving collapse of an orogenic plateau created from earlier collision and terrane accretion events in the U.S. Pacific northwest and southern British Columbia (for example, Foster and others, 2001; Butler and others, 2001; Norlander and others, 2002; Mulch and others, 2004).

The He-Pb age distributions (fig. 12) support the idea of a decoupling of crust production and exhumation in the source(s) of the OSC. Aside from a few zircons with Miocene ages for both the U/Pb and He systems and which are close to the depositional age, almost all of the He ages occupy the ~20 to 60 Ma age range that contains virtually no U/Pb ages. This decoupling of the U/Pb and He age frequency distributions is not observed in other suites of detrital zircons that we have examined. This might suggest that in the source regions of the OSC zircons such as the Cascades, southern Coast Mountains, and parts of the interior Pacific northwest, large-scale

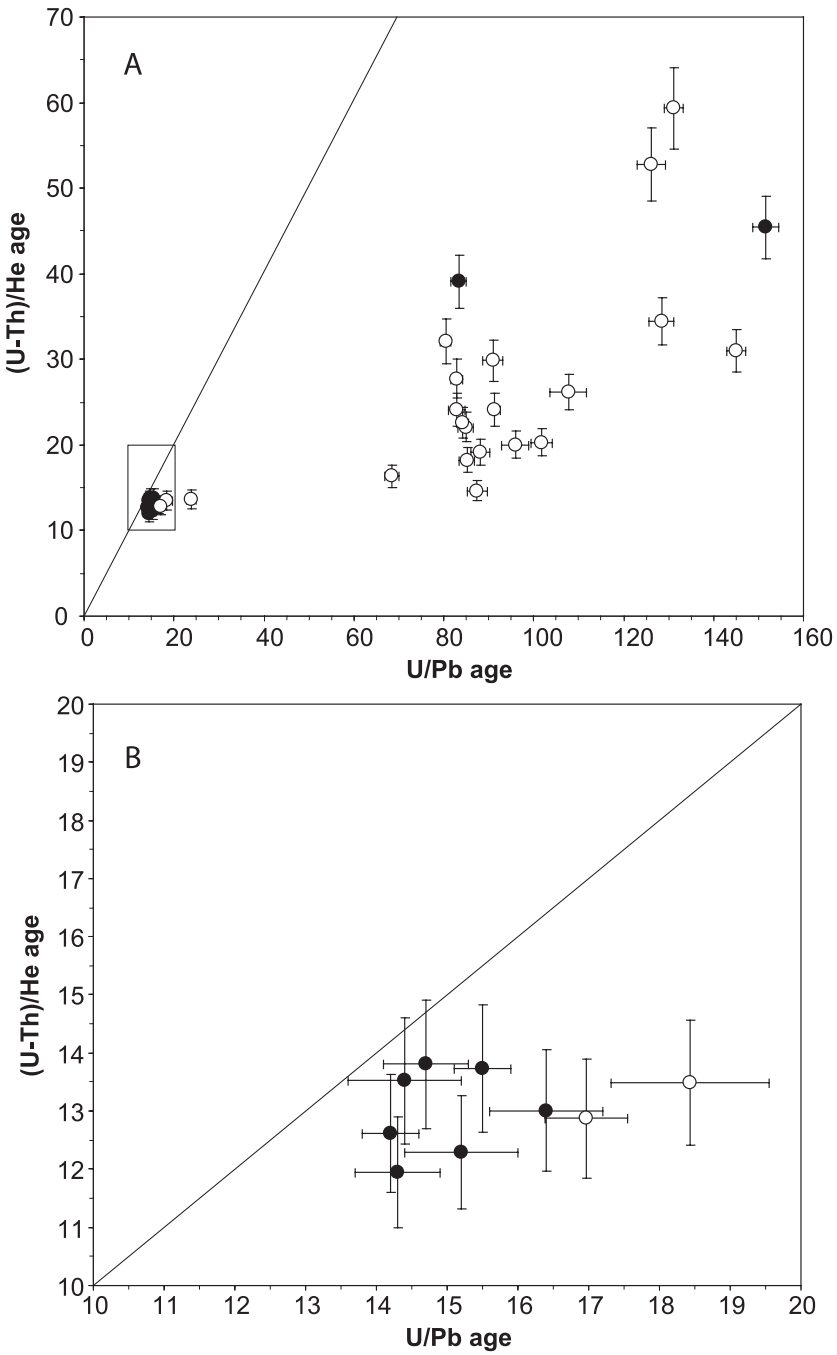

Fig. 12. He-Pb age distributions for the coastal parts of the Olympic Subduction Complex zircons. Black circles: OZ211; white circles: OZ162. Panel (B) is the close-up of the small boxed region in panel (A). All He ages range from 12 to 60 Ma. Except for samples with the youngest ages (<18 Ma), all the He ages occupy age ranges almost completely unrepresented in the U/Pb ages, possibly implying a decoupling of crustal melting/crystallization and exhumation in space and/or time in the source regions. The lack of volcanic zircons with similar He and U/Pb ages is surprising, given the essentially continuous magmatic activity of the Cascades arc since ~40 Ma. The systematically younger He ages than U/Pb ages in the youngest zircons (B), may be explained by minor partial resetting of the ZHe system in these samples. Alternatively they could indicate that either few if any of these zircons are actually volcanic (or they were inherited in their volcanic sources).

magmatism (at least of the type capable of producing zircons) was separated in space and/or time from large-scale exhumation.

Another surprising observation of the Olympic He-Pb age distribution is the scarcity of volcanic zircons. With the exception of a few of the first-cycle crystals with the youngest ages, the U/Pb and He ages of these zircons are all more than 40 Myr, or more than 50 percent of the U/Pb age, from the first-cycle volcanic trend. This result is puzzling given that the modern Cascade arc, from northern California well into British Columbia and a potential source region for at least some of the OSC sediment, has been active since ~40 Ma. As mentioned above, this could be explained by a general lack of zircons in typical arc volcanic rocks, especially of the size likely to be picked and analyzed in a detrital study such as this. It is also possible, as discussed above, that essentially all sediment in the OSC is derived from sources behind the modern Cascades arc.

A significant fraction of zircons in both samples have U/Pb ages between 14 and 16 Ma, overlapping the constraints on the depositional ages of these rocks. It might be expected that these grains are first-cycle volcanic zircons with identical crystallization and cooling ages. However, the He ages of the youngest of these grains from sample 211 are typically ~2 Myr younger than the U/Pb ages (He ages are 12 – 14 Ma, whereas the U/Pb ages are 14 – 16 Ma) and only two of the nine grains with Miocene U/Pb ages overlap the first-cycle trend at 2σ. Seven out of eight of these zircons from sample 211 possess very similar characteristics (for exampe, Th/U = 0.30 ± 0.01), suggesting derivation from the same or related magmatic systems (table 2). There is neither systematic or strong contrast between U or Th concentrations of these samples by He or U/Pb dating methods that might suggest systematic parent nuclide zonation that could influence He ages, nor is there an indication of strong zonation in the outermost few microns of the grains from LA-ICP-MS. Other potential sources of error in both He and U/Pb analyses do not point to anything allowing a systematic analytical bias of ~2 Myr in either technique.

There are two possible explanations for the fact that He ages are younger than U/Pb ages in the youngest population of zircons. One is that the cooling ages of these zircons *in their source rocks* were truly ~2 Myr younger, on average, than their crystallization ages. This possibility would mean that these sedimentary rocks are actually 12 to 14 Ma, considerably younger than the $18.3^{+3.3}_{-2.8}$ Ma suggested by the ZFT age on sample 162, but well within the 11.2 to 16.4 allowed by the foraminiferal constraints in surrounding rocks. This possibility would also mean that if these zircons are truly volcanic, they are either inherited from slightly older crustal rocks in magmatic plumbing systems, or they crystallized in a magmatic system ~2 Myr prior to eruption. In long-lived magmatic systems there may in fact be little difference between these two possibilities. Other detailed geochronologic studies of volcanic rocks have suggested age differences between zircons and other phases on the order of 100 to 700 kyr (Halliday and others, 1989; Hawkesworth and others, 2000), which is somewhat shorter than would be required in this case. But a recent high-precision U-series isotopic study of the Bergell pluton indicates a duration of time at least as long as 1.5 Myr between zircon crystallization and the end of open-system fractional crystallization, in a large crustal magma chamber (Oberli and others, 2004).

Another possible explanation for the fact that the He ages of these youngest zircons are slightly younger than the U/Pb ages is that these sedimentary host rocks experienced a post-depositional thermal history causing partial resetting of the ZHe system. Forward modeling using diffusion domains equivalent to crystal half-widths in these samples and He diffusion parameters for zircon from Reiners and others (2004) suggests that a range of thermal histories involving residence at temperatures as low as 150 °C (if held for 15 Myr, or higher temperatures for shorter durations) could reset

the ZHe ages of 15 Ma zircons to ~13 Ma. However, these thermal histories would be expected to produce stronger resetting of the AFT system and higher vitrinite reflectance values than observed for several of the nearby samples. Thus, if these zircon He ages are partially reset, then either the maximum pre-exhumation temperature has been underestimated based on AFT and vitrinite data from nearby samples, or these zircons are more susceptible to partial He loss than would be predicted by published diffusion properties for He in zircon and an assumption of equivalent crystal and diffusion domain dimensions. The extent of partial resetting required to explain these data, and its implications for the He ages of older zircons in this suite, would depend on the specific time-temperature history of the rocks. For example, if these samples cooled from partial-resetting temperatures only recently (for example, 2 – 4 Ma), then the ~2 Myr difference in He and U/Pb ages of the youngest grains could be explained by only slight resetting, whereas if the rocks cooled to low temperatures at ~13 Ma, then all of these grains could be strongly reset. These scenarios are discussed in more detail in a subsequent section.

Ukelayet flysch, Kamchatka – Partially Reset Active Margin Turbidites

The last example discussed in this paper is different from the previous ones in that there is clear evidence for extensive partial resetting of the zircon He ages. This complicates data interpretation, but provides an indication for the potential use of partially reset He ages in He-Pb double dating to constrain thermal histories of sedimentary rocks. Discussion of these data requires some consideration of previous thermochronologic results.

The Ukelayet flysch is an Upper Cretaceous-early Tertiary forearc sequence of fine- to medium-grained clastic sedimentary rocks deposited along the Cretaceous Okhotsk-Chukotka magmatic arc, which was subsequently overrun by the Upper Cretaceous Olytorsky island arc in the early Tertiary (Garver and others, 2000). Ion probe U/Pb ages of zircons from the Ukelayet flysch range from 45 Ma to 2.1 Ga, indicating a wide range of sources and a maximum depositional age of ~45 Ma (Hourigan and others, unpublished data).

Constraints on the post-depositional thermal history of the Ukelayet flysch from our study area come from fission-track dating and illite crystallinity. Detailed ZFT dating in the Ukelayet shows a range of ages between about 44 and 300 Ma. The age of the youngest peak is well correlated with stratigraphic position, varying from 88 to 44 Ma through the stratigraphic sequence and indicating nearly 40 Myr of continuous deposition (Garver and others, 2000). These data also constrain the post-depositional thermal histories to those that do not result in resetting of the ZFT thermochronometer. Broadly, this most likely means that peak burial temperatures did not exceed about 220 to 240 °C. Illite and chlorite crystallinity analysis on four of the same samples of Ukeleyat flysch that were analyzed for ZFT yielded $\Delta 2\theta$ of 0.70 to 0.80, and 0.35 to 0.42, respectively, which have been interpreted to represent maximum burial temperatures of less than 200 °C (M. Rahn, personal communication).

Apatite fission-track data are more complex than the ZFT data. The two samples analyzed for He-Pb double dating in this study, 95JG-16 and 95JG-29, yielded AFT minimum ages (see Brandon and others, 1998) of 28 ± 4 and 38 ± 11 Ma (uncertainties at 2σ), respectively. These are minimum ages and there is a wide range of grains with older unreset or partially reset ages. The fact that the samples failed the χ^2 statistical test and that one population is fully reset, indicates that each sample has experienced incomplete post-depositional resetting of the AFT system. These data have been interpreted as reflecting partial resetting of the AFT system, with full resetting of F-apatite, but partial or no resetting of the more retentive Cl-apatite. For typical Cl-apatite compositions, previously formed fission tracks will remain intact in the range of 120 C to 150 °C, but the annealing bounds of this type of apatite are not

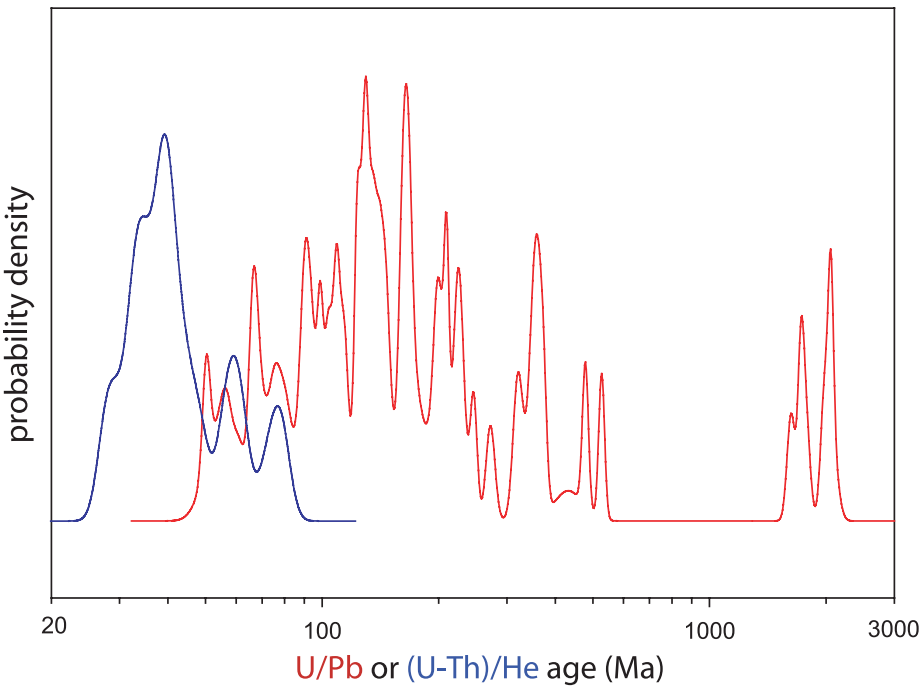

Fig. 13. Probability density plot for U/Pb and (U-Th)/He ages of zircons from the Ukelayet flysch of the Kamchatka peninsula. U/Pb ages range from 50 Ma to 2.0 Ga, with a significant gap between about 0.5 and 1.6 Ga. The largest peaks in both samples range from 90 to 160 Ma, reflecting magmatism associated with the Cretaceous arcs in this region. Minimum ages are ~50 Ma, consistent with ZFT constraints (Garver and others, 2000) suggesting a depositional age of 45 Ma. The He ages show a greatly reduced spread of ages, with a large peak at ~25 to 55 Ma, and smaller peaks centered on 60 and 80 Ma.

well studied. A recent well-constrained example in Italy suggests that tracks in Cl-apatite may be stable up to 170 °C for short heating intervals (Zattin and others, 2004). As shown below, the ZHe data on these samples are nearly (but not quite) consistent with this result because they require a maximum burial temperature, of about 160 to 170 °C.

Figure 13 shows probability densities of 67 U/Pb ages and 41 (U-Th)/He ages of zircons from the two samples studied here. U/Pb ages range from 50 Ma to 2.0 Ga, with a significant gap between about 0.5 and 1.6 Ga. The largest peaks in both samples range from 90 to 160 Ma, reflecting Cretaceous magmatism in this region (Garver and others, 2000). A related SHRIMP study of zircons from these and related samples shows very similar results (Hourigan and others, unpublished data).

Figures 13 and 14 show He probability densities and He-Pb age distributions for these samples of the Ukelayet flysch. In contrast to the ZFT ages that range from 44 to 300 Ma, the He ages show a much more restricted range, between 27 and 78 Ma, and most (74%) are less than the depositional age of 45 Ma estimated from minimum ZFT and U/Pb ages and geologic constraints. The only reasonable explanation for thermochronometric ages younger than depositional age is partial or full resetting after burial. The range of ZHe ages, along with some ages older than depositional age, indicate that post-depositional resetting was not complete. Broadly, this suggests that maximum burial temperatures likely did not exceed the nominal closure temperature for the ZHe system, ~180 °C.

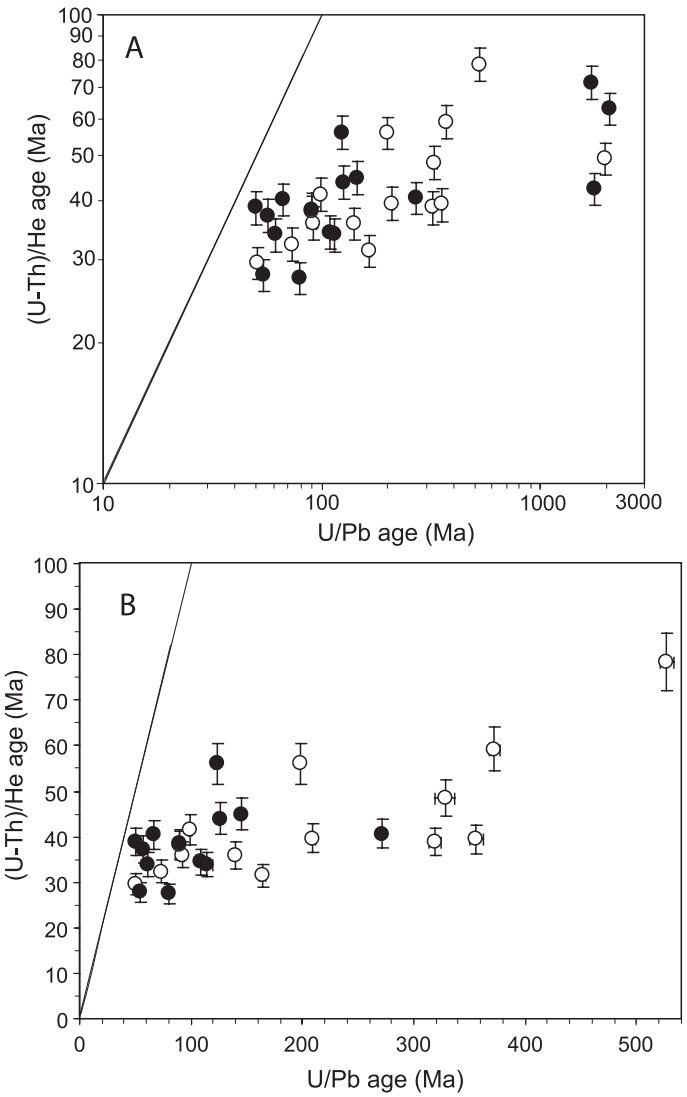

Fig. 14. He-Pb age distributions for Ukelayet flysch (Kamchatka) zircons. Panel (A) uses log scales to show all data; panel (B) shows only grains with U/Pb ages less than 550 Ma. The He ages show a much more restricted range than U/Pb ages, between 27 and 78 Ma, and most are younger than the depositional age of ~45 Ma, indicating partial resetting after burial.

If the ZHe ages were partially reset following deposition, the question arises as to why some He ages are older than others. Overall, there is only a weak correlation between U/Pb and He ages (fig. 14). Nonetheless, crystals with older U/Pb ages tend to have older He ages. This pattern of ages can be understood by considering the effects of different extents of resetting on a suite of hypothetical first-cycle volcanic zircons with different U/Pb ages. If post-depositional temperatures were sufficiently high to cause complete resetting of such a suite of zircons, the resulting post-exhumation He-Pb age distribution would form a horizontal line, with all He ages corresponding to the age of cooling through ~180 °C, regardless of the initial U/Pb

age. If post-depositional temperatures were too low to cause any He loss at all in this hypothetical first-cycle suite, the resulting distribution would form a 1:1 He-Pb age correlation. Intermediate temperatures and partial resetting would form lines of intermediate slope on such a diagram.

In reality, the distribution of He and Pb ages prior to deposition and partial resetting almost certainly did not fall entirely on the first-cycle trend. As seen in other samples that were clearly not partially reset, such as the Navajo sandstone and Mississippi River, the older the U/Pb age, the greater the likelihood that the He age is displaced farther below the first-cycle trend (that is, older grains have a greater chance of being multi-cycle). Nonetheless, this hypothetical trend of partial resetting of first-cycle zircons provides an estimate on the maximum extent of partial resetting that could have affected the suite, because a maximum extent of partial resetting can be defined for all crystals in a sample. In this case, the minimum value of partial resetting observed for any zircon in a sample defines the best estimate of maximum extent of partial resetting for all the grains in that sample.

The maximum extent of fractional partial resetting, F_r, that could have affected any crystal can be estimated by assuming that it originally had the same U/Pb and (U-Th)/He ages, and was displaced, in a plot like figure 14, to a lower He age after resetting. For simplicity we assume the time of resetting can be modeled as a discrete event ending at time t_r. The maximum fractional resetting that could have affected any individual zircon, assuming it originally lay on the first-cycle volcanic trend F_r^v, is:

$$F_r^v = 1 - \frac{t_{He} - t_r}{t_{U/Pb} - t_r} \tag{7}$$

where t_{He} and $t_{U/Pb}$ are the observed He and U/Pb ages of the zircon, respectively. The minimum F_r^v among all the zircons in a sample then defines F_r^{max}, the maximum extent of partial resetting affecting all the crystals in that sample. In this case, for an estimated age of resetting of 30 Ma (from apatite fission-track data on these samples), the minimum F_r^v, and therefore F_r^{max}, for all measured crystals from Ukelayet sample 95JG-16 is 0.56, and for sample 95JG-29 is 0.83. Thus the ZHe ages of these samples have been partially reset to maximum extents of about 60 and 80 percent, respectively. In detail, the actual fractional resetting will depend slightly on the initial He age, and the specific thermal history that results in resetting, but these are of minor concern considering the other sources of uncertainty involved.

These maximum fractional resetting estimates, and the model trends of He-Pb ages, can be forward modeled for any thermal history and He diffusion parameters using a production-diffusion model. Using a model thermal history shown in figure 15A, He-in-zircon diffusion parameters from Reiners and others (2004), and assuming effective crystal radii of 35 to 45 μm (for idealized spherical crystals, encompassing the radii of spheres with equivalent surface-area-to-volume ratios as the actual zircons in this suite), we derived the hypothetical first-cycle resetting trends shown in figure 15B. For the simplified thermal histories in figure 15, these trends provide maximum temperature estimates for the thermal histories of the Ukelayet flysch samples that range from about 160 to 170 °C. Changing the model thermal history affects the maximum burial temperature estimates, but not strongly. For example, changing the thermal history to monotonic heating and cooling trends with an infinitely short holding time at the maximum temperature, at 30 Ma, changes the maximum required temperature to ~175 to 180 °C.

SYNTHESIS AND FUTURE DIRECTIONS

Some of the original motivations for developing He-Pb double dating of detrital zircons were: a) improved resolution between candidate source terrains by more

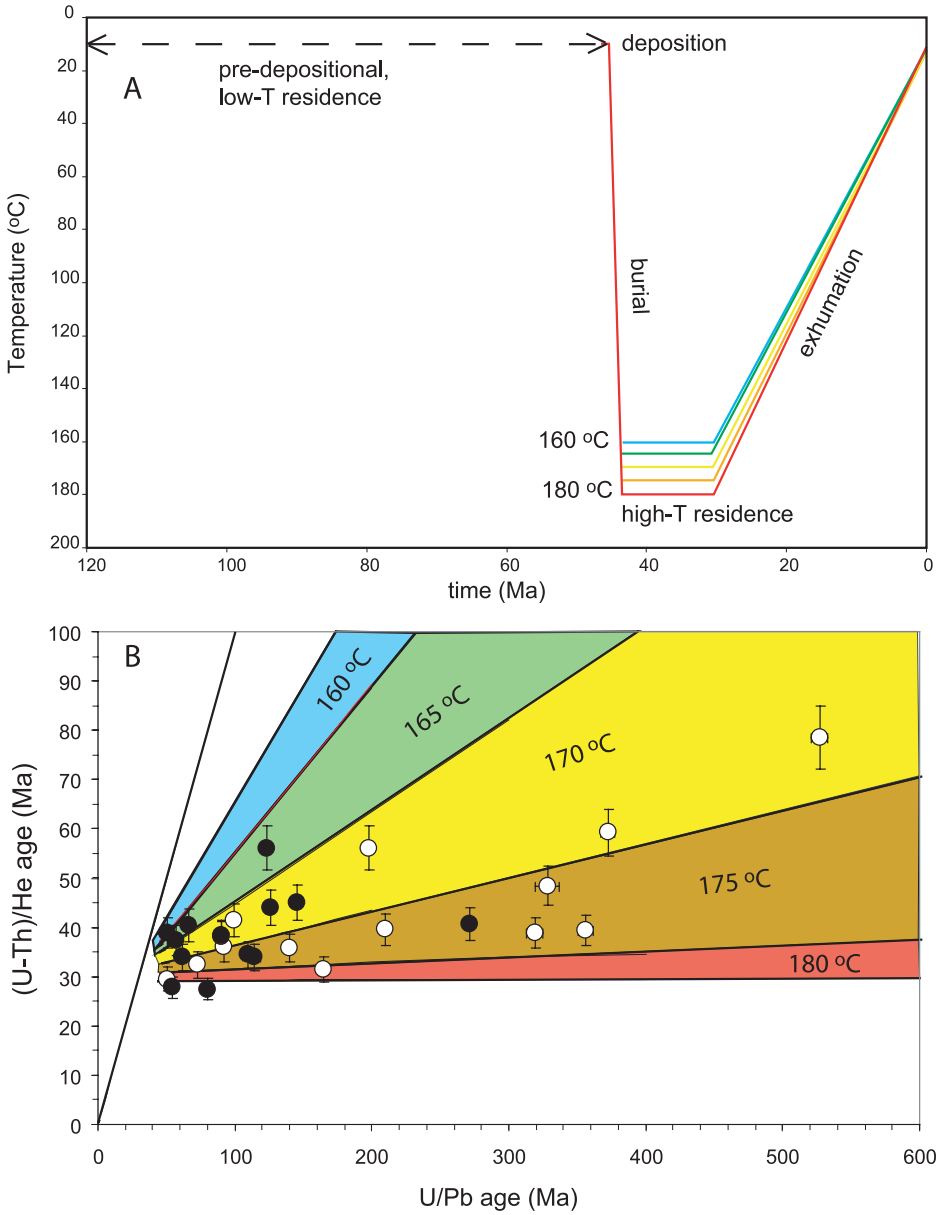

Fig. 15(A) Model thermal history for intepreting maximum burial temperatures from partially reset He ages of Ukelayet flysch (Kamchatka) zircons. The pre-depositional temperature of a zircon is assumed to be that of ambient surface (10 °C used here), since the U/Pb age. This essentially assumes that the zircon was a first-cycle volcanic zircon before deposition, placing a limit on the maximum extent of resetting. Depositional age is assumed to be 45 Ma, and heating by burial (either by superjacent deposition or thrusting) is assumed to have led to a maximum temperature by 44 Ma. The maximum temperature of 160 to 180 °C is then held until 30 Ma, at which time the unit is steadily exhumed at a constant rate. If He diffusion parameters (Reiners and others, 2004), zircon diffusion domain size (here assumed to be either 35 or 45 μm), and maximum burial temperature are held constant, then the final ZHe age will be a function of only the pre-depositional He age (that is, the U/Pb age, assuming a first-cycle volcanic zircon). (B) He-Pb age distributions in the Ukelayet samples, with fields corresponding to the maximum He age that could be observed for a given maximum burial temperature in panel (A). Each maximum temperature defines a field rather than a single line because the upper and lower bounds on

precise fingerprinting of sedimentary provenance; b) more robust constraints on depositional ages of sedimentary rocks by identification of first-cycle volcanic zircons with minimum ages; and c) improved understanding of the thermal histories of orogenic source regions. A more complete assessment of the ability of He-Pb double dating to meet these goals will have to wait for more studies and, at least in the cases of the Oregon and Olympics samples, further interpretation of the data presented here in terms of potential source regions. Nonetheless, several of these examples can be used to assess the advances in these areas.

Provenance Constraints

In provenance studies, the ability to understand both cooling age and crystal formation age provides a potentially powerful constraint on sediment provenance, especially in those cases where the potential source regions require distinctions between volcanic and slowly-cooled terrains, or between slowly-cooled terrains with distinct cooling ages. From this perspective it is not clear that any of the examples shown here demonstrate that He-Pb double dating provided key constraints that could not have come from the application of U/Pb dating alone. In the case of the Navajo sandstone, for example, Dickinson and Gehrels (2003) reached essentially the same conclusion as Rahl and others (2003), noting that the abundant Grenville U/Pb ages would be difficult to derive in significant quantities from regions other than eastern North America. Such an interpretation from U/Pb ages alone, however, would clearly make the prediction that cooling ages of most of the grains would be Paleozoic, which the double-dating results clearly confirms, making the Appalachian-derivation interpretation considerably stronger. It could also be argued, however, that a more important advantage of the double-dating approach in this case is that an Appalachian source may be more confidently concluded from analyzing significantly fewer zircons, because this combination of crystallization and cooling ages can be reasonably inferred as a characteristic of much of the Appalachians and no other large region of the continent. Thus we tentatively suggest that for source terrain characterization purposes, the combination of He and U/Pb ages on a single grain is worth many more individual U/Pb ages on other grains. Proving this statistically, however, is not straightfoward, as discussed previously.

The dominance of zircons with a western source in the Mississippi River was constrained by ZFT studies (that is low temperature cooling ages), but in this case it was only postulated that the young population (~30 Ma) represented a volcanic source (Meyer and Garver, 2000). Double dating allows a direct comparison of cooling ages and crystallization ages, and in this case demonstrated that these Oligocene cooling ages must represent a volcanic, or at least hypabyssal, source, because cooling and crystallization ages are nearly identical. This finding not only places more confidence in the western U.S. source interpretation, but also suggests that most material currently in the system is derived not from uplifted crystalline basement, but easily-eroded volcanic rocks present at relatively low local elevations throughout the western U.S. This conclusion could not be reached by AFT, ZFT or He dating alone.

We note that previous studies have shown that Th/U of zircons is often indicative of either metamorphic or igneous crystallization (for example, Williams and Claesson,

each field correspond to zircons with effective radii of 45, and 35 μm, respectively. A maximum burial temperature of 180 °C would almost completely reset all grains to the exhumation age, regardless of pre-depositional age, whereas a maximum burial temperature of 160 °C would only reset grains about 50%. The maximum observed He age at a given U/Pb age defines the minimum extent of resetting (see text), and therefore the maximum burial temperature. In this case, and for the thermal history shown in panel (A), this is about 165-170 °C.

1987; Rubatto, 2002), which may be an additional constraint on provenance of detrital grains. In particular, zircons crystallized in metamorphic environments typically have low Th/U, often less than 0.10. A survey of both bulk-grain Th/U from (U-Th)/He methods, and outer-rim Th/U from U/Pb methods show that, with rare exceptions, the zircons have Th/U between 0.1 and 1.5, consistent with crystallization from a felsic magma. Mean Th/U for all crystals except those in the Fish Canyon Tuff suite (and excluding one extreme outlier with high Th/U in Mississippi suite that probably reflects a monazite inclusion) is 0.45 ± 0.23 (one standard deviation) for bulk grains, and 0.42 ± 0.21 for their ~20-μm thick rims. Only three to five of more than 100 grains analyzed by both methods show extremely low (<0.1) or high (>1.0) Th/U. The Olympics samples in particular have a relatively restricted range of Th/U: 0.33 ± 0.09 for bulk grain and 0.29 ± 0.11 for rims, similar to that for the Oregon suite: 0.33 ± 0.13 for bulk grain and 0.40 ± 0.18 for rims. The Oregon suite is the only one containing a zircon with extremely low Th/U for both rim (0.09) and bulk grain (0.06). This zircon has a U/Pb age of 65 Ma and He age of 44 Ma. The two zircons with the lowest Th/U in the Mississippi suite (~0.28) also happen to be among the oldest: U/Pb ages of 1.0 to 1.1 Ga and He ages of 300 to 380 Ma.

Depositional Age Constraints

Attempts to constrain depositional ages by identifying the youngest He ages and first-cycle volcanic zircons were most successful in the case of the Oregon paleofluvial deposits. Although the U/Pb ages alone clearly limit the depositional age of this unit to less than 42 Ma, the identical (within error) He and U/Pb ages of this youngest zircon essentially requires that this zircon population represents a volcanic source. Perhaps more importantly, the abundant 40 to 50 Ma He ages for many more zircons with a wide range of U/Pb ages (up to 2.2 Ga) in this suite, also require a maximum depositional age of ~40 Ma.

Maximum depositional age constraints could also be derived from the minimum He ages of zircons in the Olympics samples, but the possibility of partial resetting complicates the picture. More confidence in a maximum depositional age come from the Lower Jurassic Navajo sandstone, which yielded several zircons with He ages of ~225 Ma, including those from a subset without corresponding U/Pb ages. Because the youngest U/Pb age in this unit was older than 400 Ma, and none of the Navajo zircons are first-cycle volcanic, this suggests the cooling ages provided by the He system may be more useful for constraining depositional ages in non-active margin settings.

Decoupling of Magmatism and Exhumation?

Although sediment provenance is clearly of interest, perhaps a more interesting and potentially powerful outcome of He-Pb double dating may be new, broader perspectives on the magmatic and thermal evolution of orogens, and the thermal histories of shallow crustal material over 10^8-10^9 yr timescales. These examples illustrate insights into the histories of source regions that come from comparing crystallization and cooling ages of the same single crystals.

Accepting the interpretation of an Appalachian/Caledonide source for most of the Navajo sandstone, the He-Pb age distribution of these zircons strongly suggests that most of the material shed from this Paleozoic orogen (at least that preserved in the Navajo sandstone) was actually formed in the previous orogenic episode, the Grenville Orogeny. The implication is that although extensive exhumation and cooling of rock formerly at crustal depths greater than ~6 to 9 km occurred in the Appalachian orogen, either: 1) relatively little crustal melting/crystallization occurred at this time, 2) first-cycle zircons were only produced in regions that were not exhumed during the Appalachian orogen, or 3) Appalachian drainage patterns transported first-cycle zircons towards other regions (for example, to the east, in modern coordinates).

Similar results from He-Pb double dating are also seem in the Himalayan orogen (Campbell and others, unpublished data, 2005). The first possibility might suggest that the Grenville and Appalachian orogens were fundamentally different, in that the former produced significant melting (and perhaps exhumation, as recorded by the few samples with Archean U/Pb ages with Grenville He ages), and the latter primarily exhumation with little crustal melting. The second possibility could mean that zircons produced by crustal melting in the Appalachian orogeny were confined to deeper crustal levels that will not be exposed until a subsequent orogeny affects the area. This would suggest that whereas He ages reflect the orogenic episodes contemporaneous with or closer to the age of deposition, U/Pb ages of the same zircons primarily reflect the previous orogenic episode. In other words, the characteristic depth of orogenic exhumation is greater than the closure depth of the ZHe system (~6 – 9 km), but shallower than the depth of most crustal melting and plutonic emplacement. Some evidence against the third possibility comes from examining the ages of detrital zircons in modern rivers draining the east side of the Appalachian orogen. Even in the modern east-flowing rivers, with few exceptions, the vast majority of zircons have Grenvillian U/Pb ages (Eriksson and others, 2003, 2004).

This decoupling of formation and cooling ages is perhaps clearest in the Olympic Mountains samples. Regardless of whether these zircons experienced a minor resetting event after burial, a large proportion of He ages occupy the early to middle Tertiary age range that is almost completely unoccupied by the U/Pb ages, and the U/Pb ages are almost bimodally distributed around this range. As discussed earlier, this distribution is likely due to widespread early Tertiary extension and deep exhumation of crust that was greatly thickened and magmatically active in the Cretaceous (for example, Brandon and Vance, 1992). As with the Appalachian case, it is conceivable that voluminous crustal melting accompanied the early Tertiary extension/exhumation, but if so, it was not exhumed in that orogenic event and perhaps awaits the next one.

Scarcity of First-Cycle Volcanic Zircons and Thermal History of Shallow Crustal Rocks

One somewhat surprising result of some of the examples shown here is the general scarcity of zircons with similar He and U/Pb ages that could be first-cycle volcanic zircons. None of the analyzed grains in the Navajo sandstone are first-cycle volcanic. Although both the deposits in the Olympic subduction complex and Oregon non-marine rocks were deposited within ~100 km of long-lived active magmatic regions, it is only the very youngest zircons, with ages close to depositional age, that could be first-cycle volcanic. Surprisingly, it is the Mississippi River delta sample, the one collected farthest from active magmatic regions, that contains the highest abundance of first-cycle volcanic zircons, and the only one with such zircons that have a wide range of ages, up to 105 Ma.

Assuming that these settings and our sampling of them are fairly representative of their tectonic settings, these observations may have several implications. First, continental arc settings may not necessarily produce abundant volcanic zircon. Much of the Cascade volcanic rocks may comprise relatively fine-grained intermediate to mafic rocks, for example. The Challis volcanism, interpreted to be related to a widespread thermal event in the Eocene, may also have produced dominantly andesitic volcanic rocks lacking appreciable zircon. The volcanic zircons in Mississippi River sediment may then be related to the relative abundance of rhyolitic volcanism in the Great Basin and southern Rockies, and easily eroded deposits thereof on the Great Plains. Long-lived silicic magmatic systems are known to produce considerable quantities of zircon.

A magmatic compositional control is unlikely to explain the overall lack of first-cycle volcanic zircon, however, because even though the Olympics and Oregon paleofluvial samples lack first-cycle volcanic zircons of a wide range of ages, the

youngest zircons are first-cycle volcanic. An alternative explanation for the lack of first-cycle volcanic zircons of a range of ages in these samples, compared with the Mississippi, is that zircons in active margin settings tend to recycle faster than zircons in stable interior settings. In other words, the chances of an originally volcanic zircon maintaining a He age the same as its U/Pb age decreases with age more rapidly in active margin settings because of more abundant plutonism, sedimentary or structural burial, or hydrothermal activity. Many of the zircons in the Olympics and Oregon paleofluvial deposit samples may have once been volcanic, but have since been reset by relatively vigorous tectonic and sedimentary activity. Finally, it should be mentioned again that the scarcity of first-cycle volcanic detrital zircons may be overemphasized in these examples for a variety of reasons, and that detrital grains with similar He and U/Pb ages are more abundant than these data collectively suggest. Zircon fission-track data from Kamchatka, for example, show systematically younging minimum age peaks that are consistent with U/Pb ages on other grains from the same samples (Garver and others, 2000). More work is required to determine the general abundance and distribution patterns with respect to tectonic settings of first-cycle volcanic zircons.

Partial Resetting of Zircon He Ages

The Kamchatka examples shown here, and possibly also the Olympics samples, illustrate the potential importance of partial resetting of the ZHe system in detrital samples. In the Kamchatkan case, extensive partial resetting (approximately 60 – 80%), precludes any straightforward interpretations of provenance, depositional age constraints, or thermal history of the orogenic sources of the zircons. The procedure for estimating the maximum extent of partial resetting of the zircon He ages in a sample was outlined in the section describing the Kamchatkan samples. Here we outline an approach that may be used to estimate corrections to (U-Th)/He ages for the effects of partial resetting. This involves a number of significant assumptions, including that the sample includes at least one zircon that was a first-cycle volcanic zircon prior to resetting, the ability to estimate the time elapsed since resetting (that is, the age of a hypothetical resetting event), and an accurate model for He diffusion in zircon that applies to all zircons in the sample.

Using the procedures outlined in the Kamchatka section, the maximum amount of resetting that could have affected any zircon, F_r^v, can be estimated by assuming that it was originally a first-cycle volcanic zircon (equation 7). The minimum F_r^v for all zircons in a sample then defines the maximum extent of partial resetting, F_r^{max}, that could have affected all the zircons in the sample (assuming similar He diffusion parameters and diffusion domain sizes). This approach can then be used to calculate an estimated partial-resetting-corrected zircon He age, t_{He}^{corr}:

$$t_{He}^{corr} = t_r + \frac{t_{He} - t_r}{1 - F_r^{\max}} \tag{8}$$

where t_r is the estimated age of resetting, t_{He} is the uncorrected He age, and F_r^{max} is the estimated maximum extent of fractional resetting of zircon He ages. Partial-resetting corrected ages for the Kamchatkan samples, assuming a resetting age from apatite fission-track dates of 30 Ma, are shown in figure 16. At best this approach provides only a first-order impression of what the unreset He-Pb age distribution would have been, because it assumes that all zircons were reset to the same extent, that the zircon used to define this extent originally lie on the first-cycle volcanic trend, and that the resetting event can be approximated as having a discrete age. Problems with these results can be seen in outliers with ages younger than the age of resetting, and also that several crystals have corrected ages of ~39 to 41 Ma, below the estimated age of deposition of ~45 Ma (fig. 16). These problems cannot be solved by simply changing the estimated

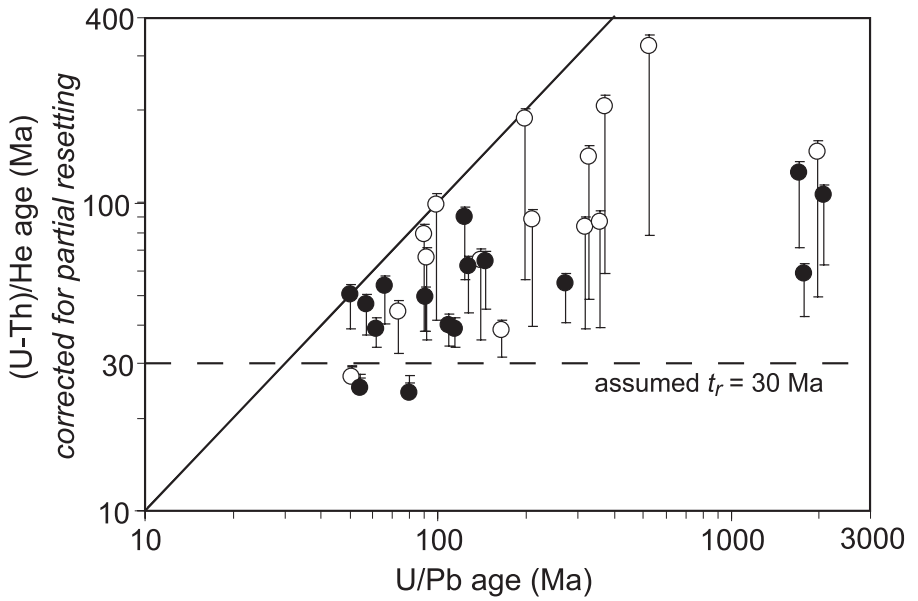

Fig. 16. He-Pb age distributions for Ukelayet flysch (Kamchatka) zircons, with He ages corrected for estimated extent of partial resetting, using the approach described in text and Equations 7 and 8. This approach uses the lowest apparent extent of partial resetting exhibited by a grain in a sample and the assumption that it was originally first-cycle volcanic (that is, same He and U/Pb ages) to estimate the maximum extent of partial resetting of all grains in the sample. It is also assumed that all grains were reset to the same extent at a certain time, t_r, which in this case is about 30 Ma, on the basis of apatite fission-track data from these samples. Crystals with uncorrected ages less than t_r (the three samples below the dashed line) do not provide meaningful results. Although there is considerable uncertainty in this correction scheme, the distribution of corrected He ages is quite similar to that of zircon fission-track ages (Garver and others, 2000), and several crystals are corrected back to the first-cycle volcanic trend, even at old ages.

age of partial resetting. Nonetheless, these results make some sense. A three-peak decomposition of these data show primary peaks at about 40 to 60 Ma, 90 to 100 Ma, and ~140 to 300 Ma, which correspond almost perfectly to the three primary P1, P2, and P3 peaks in the ZFT data (Garver and others, 2000). Also, this procedure corrects several crystals with ages as old as 200 Ma back to the first-cycle volcanic trend.

Partial-resetting corrections can also be applied to the Olympics samples to examine the effects that partial resetting may have on the observed He-Pb age distributions. In this case, the end of the possible resetting event, t_r, must be younger than the youngest zircon He age (11.9 Ma), but further constraints are difficult. The nearest sample that has been analyzed for AFT is fully reset for this system, with an AFT age of 11.7 Ma, but other nearby samples are partially reset and have minimum AFT ages of 2 to 4 Ma. In this example we assumed an estimated t_r of either 11.9 or 3 Ma. For t_r = 3 Ma, estimated maximum extent of partial resetting, F_r^{max}, for samples 211 and 162 would be 8 percent and 29 percent, respectively, whereas for t_r = 11.9 Ma, F_r^{max} would be 32 percent and 60 percent, respectively. This shows that the estimated time of resetting can have a large effect on the inferred extent of resetting, and therefore on the overall form of the He-Pb age distribution of corrected ages. Figure 17 shows estimated partial resetting corrections using the method described above, for both assumed values of t_r. For sample 162, assuming t_r = 12 Ma results in resetting-corrected ages of two of the oldest zircons moving onto or close to the first-cycle volcanic trend, whereas the youngest grains do not, and their He ages are changed significantly less by the correction. In contrast, for t_r = 3 Ma, two of the youngest zircons move onto the

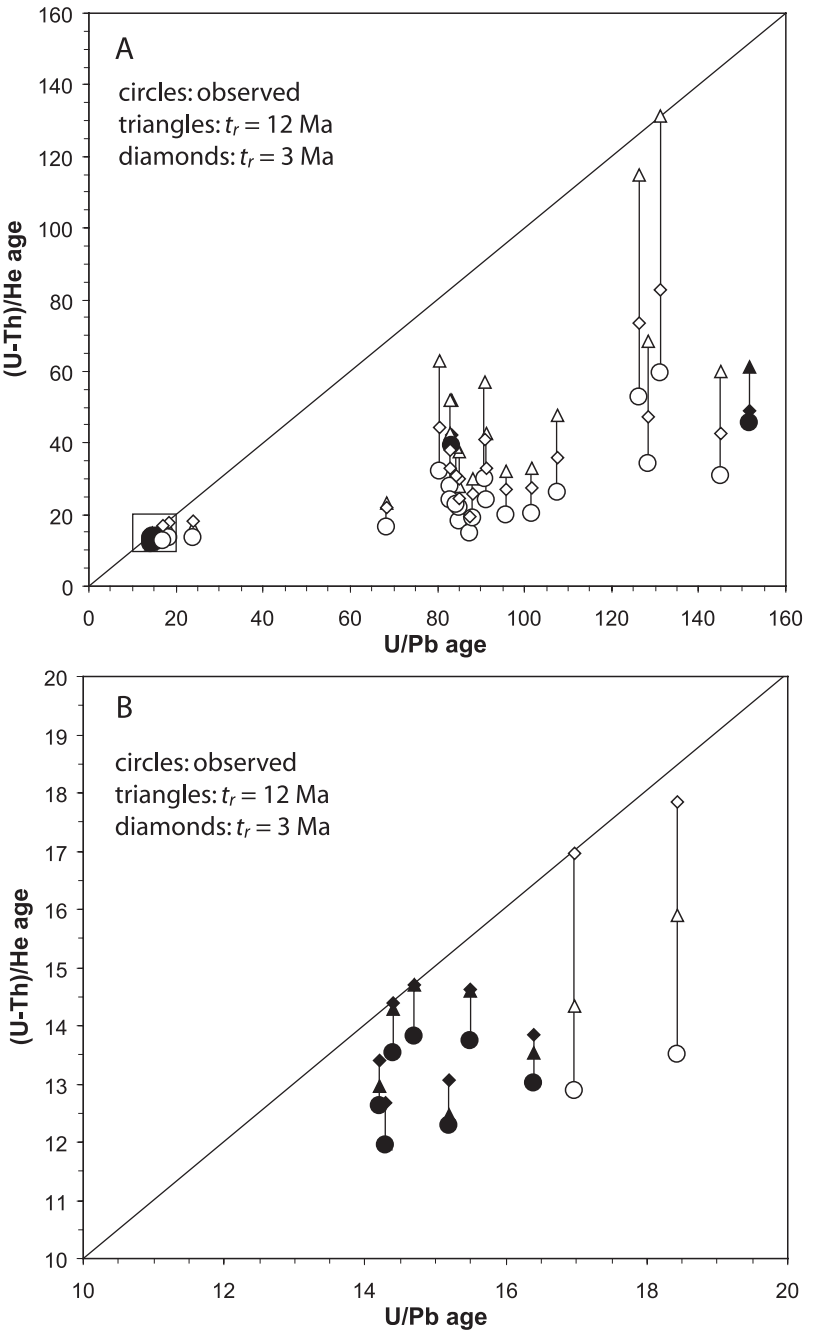

Fig. 17. Estimated corrections for hypothetical partial resetting of the Olympics samples shown in figures 11 and 12, for two different t_r, of 12 Ma (triangles) and 3 Ma (diamonds). Error bars are not shown, for clarity, though they can be seen in figure 12 for the observed data. See figure 12 and text for other details.

first-cycle volcanic trend, whereas the oldest grains are not strongly changed. Estimated age-corrections for the other sample (211) do not depend strongly on t_r, and two of the youngest samples move directly onto the first-cycle volcanic trend regardless of the assumed t_r. Although these results do not directly help constrain whether these samples are actually partially reset, or what the most realistic t_r is, they do illustrate that t_r can be important in estimating the potential impact of partial resetting on the He-Pb age distributions.

The Olympics and Kamchatkan samples were selected primarily on the basis of previous thermochronologic constraints on these or nearby samples showing unreset zircon fission-track ages (Brandon and Vance, 1992; Garver and others, 2000; Stewart and Brandon, 2004) and, more importantly, partial or mixed resetting of apatite fission-track ages, at least in nearby samples (Brandon and others, 1998; Garver, unpublished data). Although detailed thermal histories from such constraints are difficult to generalize and depend on apatite composition, for typical fluorapatite compositions this would generally be taken to indicate maximum burial temperatures less than about 120 °C. Detrital populations from quartzofeldspathic sandstones, however, typically contain apatites of a wide variety of compositions (and potentially other characteristics) that could lead to a wide variety of annealing kinetics. The examples shown here require maximum burial temperatures at least as high as about 160 °C for the Kamchatka samples, and, if the Olympics samples have been slightly reset, about 150 °C. It is beyond the scope of this paper to critically assess whether such maximum temperatures are permissible for realistic ranges of apatite compositions and annealing characteristics in detrital samples. Alternatively, it is possible that detrital zircon may experience partial resetting from thermal histories involving lower temperatures (and heating times) than predicted by assuming a simple behavior interpreted from laboratory diffusion experiments (for example, Reiners and others, 2002; Tagami and others, 2003b; Reiners and others, 2004). However, recent studies examining fossil zircon He partial retention zones in exhumed crustal blocks agree well with the laboratory data and other thermochronometeric data in the same crustal sections (Reiners and others, 2002; Tagami and others, 2003b; Stockli, 2005), and other inter-method comparisons in exhumed settings have also shown consistent results (Kirby and others, 2002; Reiners and others 2003, 2004; Stockli, 2005). Nevertheless, it could be argued that the He age profiles in exhumed crustal sections or boreholes do not directly constrain the early phases of He release from crystals with a prior long-term low-temperature history. It might be argued that radiation damage could play a role in this, because temperatures in exhumed crustal sections may be sufficiently high to prevent accumulation of damage that may cause increased diffusivity. However, we consider this unlikely, because in both the Kamchatka and Olympics cases, both the U/Pb ages and U-Th concentrations limit the maximum possible radiation dosage of each zircon, and even zircons with crystallization ages that are indistinguishable from depositional ages show features that could be interpreted as consistent with partial resetting.

From a practical perspective, attempts to use He-Pb double dating of detrital zircon for typical provenance, depositional age, or source-region thermal-history applications, should focus on units that clearly resided at temperatures below about 140 °C since deposition. Note, however, this requirement is difficult to establish with an AFT on a mixed population of grain ages because it is clearly above resetting of fluorapatite, but chlorapatite may not have been reset. As such, other indicators of thermal maturity, such as vitrinite reflectance data, could also be used. Identifying the effects of partial resetting might be difficult in many settings, especially if the depositional age of the host rock is not precisely known and the extent of partial resetting is minor, in the case of the Olympics samples. In cases of more complete

resetting, diagnosis may be possible by one or more of the following: a) ages younger than the depositional age, b) grain-size-age correlations (Reiners and Farley, 2001), or c) detection of consistently He-depleted rims of grains as shown by $^4He/^3He$ profiling (Shuster and Farley, 2004; Shuster and others, 2004).

ACKNOWLEDGMENTS

We thank J. Michael Palin for an inspirational seminar at Yale on zircon U/Pb dating by LA-ICP-MS and for some of the earliest U/Pb analyses in our efforts to develop He-Pb double dating. We thank Jeff Rahl for his work on the Navajo sandstone, Mark Brandon for helpful discussions, and George Gehrels and an anonymous reviewer for helpful reviews. This work was supported by NSF grant EAR-0236965 (PWR) and EAR-9911910 (JIG). Acknowledgment is also made to the Donors of the American Chemical Society Petroleum Research Fund for support of this research.

References

Allen, J. E., 1991, The case of the inverted auriferous paleotorrent—exotic quartzite gravels on Wallowa Mountain peaks: Oregon Geology, v. 53, p. 104–107.

Andersen, T., 2005, Detrital zircons as tracers of sedimentary provenance: limiting conditions from statistics and numerical simulation: Chemical Geology, v. 216, p. 249–270.

Armstrong, R. L., 1974, Geochronometry of the Eocene volcanic-plutonic episode in Idaho: Northwest Science, v. 3, p. 1–15.

Armstrong, R. L., Taubeneck, W. H., and Hales, P. O., 1977, Rb-Sr and K-Ar geochronometry of Mesozoic granitic rocks and their Sr isotopic composition, Oregon, Washington, and Idaho: Geological Society of America, v. 88, p. 397–411.

Bernet, M., Brandon, M. T., Garver, J. I., and Molitor, B., 2004, Fundamentals of detrital zircon fission-track analysis for provenance and exhumation studies with examples from the European Alps *in* Bernet, M., and Spiegal, C., editors, Detrital Thermochronology — Provenance analysis, exhumation, and landscape evolution of Mountain belts: Boulder Colorado: Geological Society of America Special Paper 378, p. 25–36.

Brandon, M. T., 1992, Decomposition of fission-track grain-age distributions: American Journal of Science, v. 292, p. 535–564.

——— 1996, Probability density plot for fission-track grain-age samples: Radiation Measurements, v. 26, p. 663–676.

Brandon, M. T., and Vance, J. A., 1992, Tectonic evolution of the Cenozoic Olympic subduction complex, Washington state, as deduced from fission track ages for detrital zircons: American Journal of Science, v. 292, p. 565–636.

Brandon, M. T., Roden-Tice, M. K., and Garver, J. I., 1998, Late Cenozoic exhumation of the Cascadia accretionary wedge in the Olympic Mountains, northwest Washington State: Geological Society of America Bulletin, v. 110, p. 985–1009.

Butler, R. F., Gehrels, G. E., Crawford, M. L., and Crawford, W. A., 2001, Paleomagnetism of the Quottoon plutonic complex in the Coast Mountains of British Columbia and southeastern Alaska: evidence for tilting during uplift: Canadian Journal of Earth Sciences, v. 38, p. 1367–1384.

Carter, A., and Bristow, C. S., 2000, Detrital zircon geochronology: Enhancing the quality of sedimentary source information through improved methodology and combined U-Pb and fission-track techniques: Basin Research, v. 12, p. 47–57.

Cisneros, G., 1999, Reconstruction of a Late Cretaceous-Paleocene river system—Geometry of an Eartly Tertiary nonconformity in the Elkhorn Mountains, northeastern Oregon, *in* Mendelson, C.V., and Mankiewicz, C. (compilers), 12th Keck Research Symposium in Geology, Proceedings: Northfield, Minnesota, Fairway Foods, p. 291–294.

Clark, J., Beerbower, J. R., and Kietzke, K. K., 1967, Oligocene and sedimentation, stratigraphy, paleoecology and paleoclimatology in the Big Badlands of South Dakota: Fieldiana Geological Memoirs, v. 5, 158 p.

Cumming, G. L., and Richards, J. R., 1975, Ore lead isotope ratios in a continuously changing earth: Earth and Planetary Science Letters, v. 28, p. 155–171.

Dickinson, W. R., and Gehrels, G. E., 2003, U–Pb ages of detrital zircons from Permian and Jurassic eolian sandstones of the Colorado Plateau, USA: paleogeographic implications: Sedimentary Geology, v. 163, p. 29–66.

Dodson, M. H., 1986, Closure profiles in cooling systems: Materials Science Forum, v. 7, p. 145–154.

Dodson, M. M., Compston, W., Williams, I. S., and Wilson, J. F., 1988, A search for ancient detrital zircons in Zimbabwean sediments: Journal of the Geological Society of London, v. 145, p. 977–983.

Eriksson, K. A., Campbell, I. H., Palin, J. M., and Allen, C. M., 2003, Predominance of Grenvillian magmatism recorded in detrital zircons from modern Appalachian rivers: Journal of Geology, v. 111, p. 707–717.

Eriksson, K. A., Campbell, I. H., Palin, J. M., Allen, C. M., and Bock, B., 2004, Evidence for multiple recycling in Neoproterozoic through Pennsylvanian sedimentary rocks of the central Appalachian Basin: Journal of Geology, v. 112, p. 261–276.

Ewing, R. C., Meldrum, A., Wang, L., Weber, W. J., and Corrales, L. R., 2003, Radiation effects in zircon: Reviews in Mineralogy and Geochemistry, v. 53, p. 387–425.
Farley, K. A., 2002, (U-Th)/He dating: Techniques, calibrations, and applications: Mineralogical Society of America, Reviews in Mineralogy and Geochemistry, v. 47, p. 819–844.
Farley, K. A., Wolf, R. A., Silver, L. T., 1996, The effects of long alpha-stopping distances on (U-Th)/He ages: Geochimica et Cosmochimica Acta, v. 60, p. 4223–4229.
Fedo, C. M., Sircombe, K. N., and Rainbird, R. H., 2003, Detrital zircon analysis of the sedimentary record, in Zircon: Reviews in Mineralogy and Geochemistry, v. 53, p. 277–298.
Foster, D. A., and Fanning, C. M., 1997, Geochronology of the northern Idaho Batholith and the Bitterroot metamorphic core complex; magmatism preceding and contemporaneous with extension: Geological Society of America Bulletin, v. 109, p. 379–394.
Foster, D. A., Schafer, C., Fanning, C. M., and Hyndman, D. W., 2001, Relationships between crustal partial melting, plutonism, orogeny, and exhumation: Idaho-Bitterrot batholith: Tectonophysics, v. 342, p. 313–350.
Frazier, W. J., and Schwimmer, D. R., 1987, Regional stratigraphy of North America: New York, New York, Plenum Press, 719 p.
Garver, J. I., and Kamp, P. J. J., 2002, Integration of zircon color and zircon fission track zonation patterns in orogenic belts: Application of the Southern Alps, New Zealand: Tectonophysics, v. 349, p. 203–219.
Garver, J. I., Soloviev, A.V., Bullen, M. E., and Brandon, M. T., 2000, Towards a more complete record of magmatism and exhumation in continental arcs, using detrital fission-track thermochronometry: Physics and Chemistry of the Earth Part A, v. 25, p. 565–570.
Garver, J. I., Reiners, P. W., Walker, L. J., Ramage, J. R., and Perry, S. E., 2005, Implications for timing of Andean uplift based on thermal resetting of radiation-damaged zircon in the Cordillera Huayhuash, northern Perú: Journal of Geology, v. 113, p. 117–138.
Halliday, A. N., Mahood, G. A., Holden, P., Metz, J. M., Dempster, T. J., and Davidson, J. P., 1989, Evidence for long residence times of rhyolitic magma in the Long Valley magmatic system—The isotopic record in precaldera lavas of Glass Mountain: Earth and Planetary Science Letters, v. 94, p. 274–290.
Hamilton, W., and Myers, W. B., 1974, Nature of the Boulder Batholith of Montana: Geological Society of America Bulletin, v. 85, p. 365–378.
Hawkesworth, C. J., Blake, S., Evans, P., Hughes, R., MacDonald, R., Thomas, L. E., Turner, S. P., and Zellmer, G., 2000, Time scales of crystal fractionation in magma chambers—Integrating physical, isotopic and geochemical perspectives: Journal of Petrology, v. 41, p. 991–1006.
Heimlich, R. A., and Armstrong, R. L., 1972, Variance of Precambrian K-Ar biotite dates, Bighorn Mountains, Wyoming: Earth and Planetary Science Letters, v. 14, p. 75–78.
Heimlich, R. A., and Banks, P. O., 1968, Radiometric age determinations, Bighorn Mountains, Wyoming: American Journal of Science, v. 266, p. 180–192.
Holland, H. D., and Gottfried, D., 1955, The effect of nuclear radiation on the structure of zircon: Acta Crystallographica, v. 8, p. 291–300.
Hourigan, J. K., Reiners, P. W., and Brandon, M. T., 2005, U-Th zonation dependent alpha-ejection correction in (U-Th)/He chronometry, Part I: Theory: Geochimica et Cosmochimica Acta, v. 69, p. 3349–3365.
House, M. A., Farley, K. A., and Stockli, D., 2000, Helium chronometry of apatite and titanite using Nd-YAG laser heating: Earth and Planetary Science Letters, v. 183, p. 365–368.
Hurley, P. M., 1954, The helium age method and the distribution and migration of helium in rocks, *in* Faul, H., editor, Nuclear Geology: New York, Wiley, p. 301–329.
Hurley, P. M., Larsen, E. S., Jr., and Gottfried, D., 1956, Comparison of radiogenic helium and lead in zircon, Geochimica et Cosmochimica Acta, v. 9, p. 98–102.
Hurley, P. M., Brookins, D. G., Pinson, W. H., Hart, S. R., and Fairbairn, H. W., 1961, K-Ar age studies of Mississippi and other river sediments: Geological Society of America Bulletin, v. 72, p. 1807–1816.
Janeke, S. U., and Snee, L. W., 1993, Timing and episodicity of middle Eocene volcanism and onset of conglomerate deposition, Idaho: Journal of Geology, v. 101, p. 603–621.
Jennison, M. J., ms, 1980, Zircon ages and feldspar mineralogy of the Navajo Sandstone: MS Thesis, Department of Geology and Geophysics, University of Utah, 76 p.
Kinny, P. D., and Maas, R., 2003, Lu-Hf and Sm-Nd isotope systematics in zircon, in Zircon: Reviews in Mineralogy and Geochemistry, v. 53, p. 327–341.
Kirby E., Reiners, P. W., Krol, M., Hodges, K., Farley, K. A., Whipple, K., Yiping, L., Tang, W., and Chen, Z., 2002, Late Cenozoic uplift and landscape evolution along the eastern margin of the Tibetan plateau: Inferences from $^{40}Ar/^{39}Ar$ and U-Th-He thermochronology: Tectonics, v. 21, n. 1, 10.1029/2000TC001246.
Kocurek, G., and Dott, R. J., Jr., 1983, Jurassic paleogeography and paleoclimate of the central and southern Rocky Mountains region, *in* Reynolds, M. W., and Dolly, E. D., editors, Mesozoic paleogeography of the west-central United States: Denver, Colorado, Rocky Mountain Section, Society of Economic Paleontologists and Mineralogists, Rocky Mountain Paleogeography Symposium 2, p. 101–116.
Lanphere, M. A., and Baadsgaard, H., 2001, Precise K-Ar, $^{40}Ar/^{39}Ar$, Rb-Sr and U/Pb mineral ages from the 27.5 Ma Fish Canyon Tuff reference standard: Chemical Geology, v. 175, p. 653–671.
Lipman, P. W., Steven, T. A., and Mehnert, H. H., 1970, Volcanic history of the San Juan Mountains, Colorado, as indicated by potassium-argon dating: Geological Society of America Bulletin, v. 81, p. 2329–2352.
Lipman, P. W., Doe, B. R., Hedge, C. E., and Steven, T. A., 1978, Petrologic evolution of the San Juan volcanic field, southwestern Colorado: Pb and Sr isotope evidence: Geological Society of America Bulletin, v. 89, p. 59–82.

Marzolf, J. E., 1988, Controls on late Paleozoic and early Mesozoic eolian deposition of the western United States: Sedimentary Geology, v. 56, p. 167–191.
Meyer, N. M., ms, 2000, Fission-track ages of detrital zircon from the Mississippi and Colorado Rivers: Unpublished senior thesis, Union College, Schenectady, New York.
Meyer, N. R., and Garver, J. I., 2000, Zircon fission-track fingerprint of major tributaries to the Mississippi River: Geological Society of America Abstracts with Program, v. 32, n. 1, p. 59.
Mulch, A., Teyssier, C., Cosca, M. A., Vanderhaeghe, O., and Vennemann, T. W., 2004, Reconstructing paleoelevation in eroded orogens: Geology, v. 32, p. 525–528.
Naeser, N. D., Naeser, C. W., Morgan, B. A., III, Schultz, A. P., and Southworth, C. S., 2000, Paleozoic to Recent cooling history of the Appalachian Blue Ridge Province in North Carolina, Tennesse, and Virginia, eastern United States, from apatite and zircon fission track analysis: Geological Society of Australia Abstracts Series, v. 58, p. 237.
Nasdala, L., Wenzel, M., Vavra, G., Irmer, G., Wenzel, T., and Kober, B., 2001, Metamictisation of natural zircon: accumulation versus thermal annealing of radioactivity-induced damage: Contributions to Mineralogy and Petrology, v. 141, p. 125–144.
Nasdala, L., Reiners, P. W., Garver, J. I., Kennedy, A. K., Stern, R. A., Balan, E., and Wirth, R., 2004, Incomplete retention of radiation damage in zircon from Sri Lanka: American Mineralogist, v. 89, p. 219–231.
Norlander, B. H., Whitney, D. L., Teyssier, C., and Vanderhaeghe, O., 2002, Partial melting and decompression of the Thor-Odin dome, Shuswap metamorphic core complex, Canadian Cordillera: Lithos, v. 61, p. 103–125.
Oberli, F., Meier, M., Berger, A., Rosenberg, C. L., and Giere, R., 2004, U-Th-Pb and $^{230}Th/^{238}U$ disequilibrium isotope systematics: Precise accessory mineral chronology and melt evolution tracing in the Alpine Bergell intrusion: Geochimica et Cosmochimica Acta, v. 68, p. 2543–2560.
Patchett, J. P., Ross, G. M., and Gleason, J. D., 1999, Continental Drainage in North America During the Phanerozoic from Nd Isotopes: Science, v. 283, p. 671–673.
Peterson, F., 1988, Pennsylvanian to Jurassic eolian transportation systems in the western United States: Sedimentary Geology, v. 56, p. 207–260.
Rahl, J. M., Reiners, P. W., Campbell, I. H., Nicolescu, S., and Allen, C. M., 2003, Combined single-grain (U-Th)/He and U/Pb dating of detrital zircons from the Navajo Sandstone, Utah: Geology, v. 31, p. 761–764.
Rahn, M. K., Brandon, M. T., Batt, G. E., and Garver, J. I., 2004, A zero-damage model for fission-track annealing in zircon: American Mineralogist, v. 89, n. 3, p. 473–484.
Reiners, P. W., and Farley, K. A., 2001, Influence of crystal size on apatite (U-Th)/He thermochronology: An example from the Bighorn Mountains, Wyoming: Earth and Planetary Science Letters, v. 188, p. 413–420.
Reiners, P. W., Farley, K. A., and Hickes, H. J., 2002, He diffusion and (U-Th)/He thermochronometry of zircon: Initial results from Fish Canyon Tuff and Gold Butte, Nevada: Tectonophysics, v. 349, p. 297–308.
Reiners, P.W., Zhou, Z., Ehlers, T. A., Xu, C., Brandon, M.T., Donelick, R. A., and Nicolescu, S., 2003, Post-orogenic evolution of the Dabie Shan, eastern China, from (U-Th)/He and fission-track dating: American Journal of Science, v. 303, p. 489–518.
Reiners, P. W., Spell, T. L., Nicolescu, S., and Zanetti, K. A., 2004, Zircon (U-Th)/He thermochronometry: He diffusion and comparisons with $^{40}Ar/^{39}Ar$ dating: Geochimica et Cosmochimica Acta, v. 68, p. 1857–1887.
Roden, M. K., Elliott, W. C., Aronson, J. L., and Miller, D. S., 1993, A comparison of fission-track ages of apatite and zircon to the K/Ar ages of illite/smectite (I/S) from Ordovician K-Bentonites, Southern Appalachian Basin: Journal of Geology, v. 101, p. 633–641.
Rubatto, D., 2002, Zircon trace element geochemistry: Partitioning with garnet and the link between U-Pb ages and metamorphism: Chemical Geology, v. 184, p. 123–128.
Sambridge, M. S., and Compston, W., 1994, Mixture modelling of multi-component data sets with application to ion-probe zircon ages: Earth and Planetary Science Letters, v. 128, p. 373–390.
Schmitz, M. D., and Bowring, S. A., 2001, U-Pb zircon and titanite systematics of the Fish Canyon Tuff: an assessment of high precision U-Pb geochronology and its application to young volcanic rocks: Geochimica et Cosmochimica Acta, v. 65, p. 2571–2587.
Schmitz, M. D., Bowring, S. A., Ludwig, K. R., and Renne, P. R., 2003, Comment on "Precise K-Ar, $^{40}Ar^{39}Ar$, Rb-Sr and U-Pb mineral ages from the 27.5 Ma Fish Canyon Tuff reference standard" by M. A. Lanphere and H. Baadsgaard: Chemical Geology, v. 199, p. 277–280.
Shuster, D. L., and Farley, K. A., 2004, $^{4}He/^{3}He$ thermochronometry: Earth and Planetary Science Letters, v. 217, p. 1–17.
Shuster, D. L., Farley, K. A., Sisterson, J. M., and Burnett, D. S., 2004, Quantifying the diffusion kinetics and spatial distributions of radiogenic ^{4}He in minerals containing proton-induced ^{3}He: Earth and Planetary Science Letters, v. 217, p. 19–32.
Sircombe, K. N., 2000, Quantitative comparison of geochronological data using multivariate analysis: a provenance study example from Australia: Geochimica et Cosmochimica Acta, v. 64, p. 1593–1619.
Sircombe, K. N., and Hazelton, M. L., 2004, Comparison of detrital zircon age distributions by kernel functional estimation: Sedimentary Geology, v. 171, p. 91–111.
Snavely, P. D., Jr., and Kvenvolden, K. A., 1989, Preliminary evaluation of the petroleum potential of the Tertiary accretionary terrane, west side of the Olympic Peninsula, Washington: A. Geology and hydrocarbon potential: U.S. Geological Survey Bulletin 1892, p. 1–17.
Soloviev, A.V., Shapiro, M. N., Garver, J. I., Scherbinina, E. A., and Kravchenko-Berezhnoy, I. R., 2002, New age data from the Lesnaya Group: a key to understanding the timing of arc-continent collision, Kamchatka, Russia: Island Arc, v. 11, p. 79–90.

Stearns, H. T., 1954, Evidence of a missing Lower Paleozoic (?) Formation in the Hells Canyon area, Idaho-Oregon: Bulletin of the Geological Society of America, v. 65, p. 939.
Steven, T. A., 1975, Mid-Tertiary volcanic field in the southern Rocky Mountains: Geological Society of America Memoir 144, p. 75–94.
Stewart, R. J., and Brandon, M. T., 2004, Detrital-zircon fission-track ages for the "Hoh Formation": Implications for late Cenozoic evolution of the Cascadia subduction wedge: Geological Society of America Bulletin, v. 116, p. 60–75.
Stockli, D., 2005, Thermochronometry of extensional settings, *in* Reiners, P. W., and Ehlers, T. A., editors, Thermochronometry: Reviews in Mineralogy and Geochemistry.
Sweetkind, D. S., and Blackwell, D. D., 1989, Fission-track evidence of the Cenozoic thermal history of the Idaho batholith: Tectonophysics, v. 157, p. 241–250.
Tagami, T., Farley, K. A., and Stockli, D. F., 2003a, (U-Th)/He geochronology of single zircon grains of known Tertiary eruption age: Earth and Planetary Science Letters, v. 6531, p. 1–11.
Tagami, T., Farley, K. A., and Stockli, D. F., 2003b, Thermal sensitivities of zircon (U-Th)/He and fission-track systems, [abs., 2003 Goldschmidt Conference]: Geochimica et Cosmochimica Acta, v. 67, n. 18(S1), p. A466.
Taubeneck, W. H., 1955, Age of the Bald Mountain batholith, northeastern Oregon: Northwest Science, v. 29, p. 93–96.
Toth, M. I., and Stacey, J. S., 1992, Constraints on the formation of the Bitterroot Lobe of the Idaho Batholith, Idaho and Montana, from U-Pb zircon geochronology and feldspar Pb isotopic data: U.S. Geological Survey Bulletin B2008, 14 p.
Trafton, K. S., 1999, Paleogeographic implications of Late Cretaceous-Early Tertiary quartzite-bearing fluvial sediments, Elkhorn Mountains, Northeast Oregon, *in* Mendelson, C. V., and Mankiewicz, C. (compilers), 12th Keck Research Symposium in Geology, Proceedings: Northfield, Minnesota, Fairway Foods, p. 287–290.
Valley, J. W., 2003, Oxygen isotopes in zircon, *in* Hanchar, J. M., and Hoskin, P. W. O., editors, Zircon: Reviews in Mineralogy and Geochemistry, v. 53, p. 343–385.
Vermeesh, P., 2004, How many grains are needed for a provenance study?: Earth and Planetary Science Letters, v. 224, p. 441–451.
Williams, I. S., and Claesson, S., 1987, Isotopic evidence for the Precambrian provenance and Caledonian metamorphism of high grade paragneisses from the Seve Nappes, Scandinavian Caledonides: II. Ion-microprobe zircon U-Th-Pb: Contributions to Mineralology and Petrology, v. 97, p. 205–217.
Zattin, M., Aldega, L., Bersani, D., Corrado, S, Invernizzi, C., and Mazzoli, S., 2004, Multidisciplinary constraints to the apatite annealing temperatures: a case history from the southern Apennines: Amsterdam, 10th International Fission track conference, Abstract volume, p. 50.
Zhang, M., Salje, E. K. H., Farnan, I., Graeme-Barber, A., Daniel, P., Ewing, R. C., Clark, A. M., and Lennox, H., 2000, Metamictization of zircon: Raman spectroscopic study: Journal of Physics: Condensed Matter, v. 12, p. 1915–1925.